Journal of Hydrology: Regional Studies 29 (2020) 100685

Contents lists available at ScienceDirect

Journal of Hydrology: Regional Studies

journal homepage: www.elsevier.com/locate/ejrh

Evaluating a parsimonious watershed model versus SWAT to estimate streamflow, soil loss and river contamination in two case studies in Tietê river basin, São Paulo, Brazil

Franciane Mendonça dos Santos[a,b,*], Rodrigo Proença de Oliveira[b], Frederico Fábio Mauad[c]

[a] São Carlos School of Engineering, SP, Center of Water Resourses and Environmental Studies, University of São Paulo, Brazil
[b] CERIS, Civil Engineering Research and Inovation for Sustainability, Instituto Superior Técnico, Universidade de Lisboa, Av. Rovisco Pais, 1049-001, Lisboa, Portugal
[c] São Carlos School of Engineering, Center of Water Resourses and Environmental Studies, University of São Paulo, Caixa Postal 292, São Carlos, SP, CEP: 13560-970 Brazil

ARTICLE INFO

Keywords:
SWAT
GWLF
Parsimonious lumped hydrological model
Distributed hydrological model

ABSTRACT

Study region: The Atibaia and Jacaré-Guaçu watersheds from the Tietê river basin, São Paulo, Brazil.
Study focus: This study aims to compare estimates of flow, sediment yield and nutrients loads obtained from two distinct models with different structures and degree of complexity. The Generalized Watershed Loading Function (GWLF) and the Soil Water Assessment Tool (SWAT). We are particularly interested in understanding under which conditions the use of each model is to be recommended, namely when does the addition effort required to run the SWAT model leads to effective better results. As SWAT's calibration procedure is cumbersome, the advantage of using a more detailed and distributed model fails to materialize when detailed data are not available or when monthly estimates are enough. GWLF model provides useful results with a reduced data gathering and calibration effort.
New hydrological insights of the region: The joint calibration of both models to two watersheds offered a robust set of parameter values for prevalent conditions of Tiête river basin given the existing data set, although not all modelled variables are reproduced accurately. The performance of both models is adequate when estimating streamflow at a monthly time, but decreases when estimating daily flow, sediment yield, and nutrients loads. The poor monitoring of sediments and nutrients concentration hinders the ability to fully calibrate the model's water quality component.

1. Introduction

Understanding and evaluating the natural processes occurring in a watershed are continuing challenges for scientists and engineers who often struggle with lack of data, as long-term watershed monitoring efforts are difficult to maintain due to its cost, especially the ones aimed at sediment transport and water quality. The use of mathematical models to simulate hydrological

* Corresponding author at: São Carlos School of Engineering, SP, Center of Water Resourses and Environmental Studies, University of São Paulo, Brazil.
E-mail address: franciane.mds@usp.br (F.M.d. Santos).

https://doi.org/10.1016/j.ejrh.2020.100685
Received 18 March 2019; Received in revised form 19 March 2020; Accepted 19 March 2020

processes, including water quality, is a possible solution to overcome this problem and to extrapolate conclusions from the existing data (Mirchi et al., 2010; Hajigholizadeh et al., 2018).

Historically, different types of models have been applied to estimate streamflow, determine pollution loads and to derive pollutant concentrations in streams and other water bodies. Watershed models now include these modelling components in a single computer code and can calculate the stream flow and their associated sediment and pollutant loads from meteorological data and land use data. Water managers use them to evaluate the impacts of climate and land use change on stream flow and water quality and to assess the efficacy of conservation practices (Quilbé et al., 2006; Devia et al., 2015).

The prediction accuracy of each model depends on the model structure, availability and quality of input data as well as model parameter values that must be estimated. Physically based and distributed watershed models that detail the hydrological process occurring in the basin have the potential to be able to reproduce the space-time varying fluxes of water and contaminants at various watersheds, climates and hydrological environments. In principle, true physically based models can be used without calibration because their parameters have a physical meaning that can be measured in nature. In practice, calibration is usually required because measurements are not available for all parameters at all locations and because there are no completely physically based model and all have at a few empirical approximations that require calibration (Beven, 2001).

The potential robustness and accuracy of distributed physically based models have a strong appeal to water managers that need to preview future conditions and make decisions under different scenarios. Although, these complex watershed models require a large data and parameter set to characterize the river basin and its hydrological processes, the increase of computer power and the advent of geographic information systems have facilitated their use and led to a tendency of using increasingly complex models. The SWAT model is one of such examples, with more than 2100 references in scientific journals (Francesconi et al., 2016). Several authors have questioned this approach and have shown that simpler and more conceptual models, requiring less data, are almost as accurate as complex ones and can explain much of the observed values variance, and that both simple and complex models will perform poorly in certain cases (Naef, 1981; Wilcox et al., 1990; Michaud and Sorooshian, 1994; Ajami et al., 2004; Gupta et al., 2008; Fatichi et al., 2016).

A guiding principle when selecting a model is to find the least complex model that will solve the problem under analysis with the available data. This idea is a corollary of the XIII century Ocham's principle that states that any unnecessary complexity should be avoided and has been reinforced by several authors that argue for the need to balance parsimony and complexity when selecting a hydrological model (Young et al., 1996; Fatichi et al., 2016).

Another inherent problem of complex distributed watershed models with a large parameter set is their calibration and validation procedures and issues related parameter uncertainty, overfitting and equifinality (Beven, 2001). To overcome these problems large datasets are needed with a large enough amount of information to enable the identification of the appropriate values to assign to each model parameter. The calibration and validation of complex distributed models becomes a cumbersome procedure that requires experienced users, as unexperienced users are prone to failure or even to error.

In this work, we compared the results from a lumped-parameter model with parsimonious data requirements, the Generalized Watershed Loading Function (GWLF) (Haith and Shoemaker, 1987), with those obtained by Soil Water and Assessment Tool (SWAT) (Arnold et al., 1998: Arnold and Fohrer, 2005), a semi-distributed model with large data requirements. The literature reports several applications of GWLF, namely in the United States of America (Haith et al., 1992; Swaney et al., 1996; Lee et al., 2000; Schneiderman et al., 2002; Tu et al., 2009; Li et al., 2010; Niraula, 2013), China (Huang and Hong, 2010; Du et al., 2014) and in Porto Rico (Wu et al., 2007). SWAT has more than 2100 references in scientific journals (Francesconi et al., 2016). It is our understanding that GWLF has never been applied to Brazil case studies and that the number of SWAT applications for sediment and nutrients load prediction is limited. Given the scale of the country and the scarcity of monitoring data for such large area, research is needed on the implications of spatial and temporal resolution on modelling results.

Previous studies have compared distinct watershed models with different structures and complexity (Wilcox et al., 1990; Michaud and Sorooshian, 1994; Parajuli et al., 2009; Li et al., 2010; Li and Xu, 2011; Caldwell et al., 2015), focusing mainly on the models' ability to reproduce streamflow, not evaluating their performance of estimating sediment yield and nitrogen and phosphorus loads. Additionally, although physically-based models can be used in a daily step, most of these papers perform and discuss the model calibration at a monthly time step and do not discuss the difficulty of reproducing daily values of flow, sediment and nutrient loads. Parajuli et al (2009) compared the hydrology, sediments and total phosphorus simulation results of AnnAGNPS (Annualized Agricultural Non-Point Source model) and SWAT models. Both models provided fair to very good estimates of the monthly streamflow and sediment yield and SWAT performed consistent well in reproducing total phosphorus. Niraula (2013) used SWAT and GWLF to identify the areas contributing the most to the pollution problems of 570 km^2 watershed in Alabama, United States. The authors compared the model' results at a monthly time scale and concluded that, while both models perform well for streamflow, SWAT performed slightly better for sediment, nitrogen and phosphorus. Qi et al (2017) compared SWAT and GWLF monthly estimates of flow, sediment and nitrogen loads for two watersheds in China, with different climatic conditions. Both models performed similarly well in reproducing streamflow and sediment, but the results were inconsistent for nitrogen.

This study evaluates the ability GWLF and SWAT to predict the daily and monthly variation of streamflow, sediment yield, total nitrogen load and total phosphorus load in the streams of two watersheds in Tietê river basin, in São Paulo, Brazil. Initial model runs immediately indicated that both models needed calibration.

A growing of published research discusses the challenges and possible solutions to calibrate distributed watershed models (e.g., Madsen, 2000; Gupta et al., 2008; Yilmaz et al., 2008). The results from this research are particular important for calibrating distributed models with a high number of parameters, like SWAT, where a manual approach is a cumbersome process which often leads to poor results. However, as our research focus was the comparison of two models, a careful manual calibration had the

advantage of providing insights to the role of each parameter and identifying links between the parameters of both models.

Both models were simultaneously calibrated and validated for two river basins, using split samples from different monitoring records stations in the two watersheds (Klemeš, 1986). SWAT and GWLF share some steps in their modelling approach and several parameters. As the model's parameters depend on the physical characteristics of the river basin, in our study, shared parameters have been assigned the same values and others which measure similar concepts have been assigned compatible values. The joint calibration of both models to two watersheds offers a way to find a robust set of parameter values for the prevalent conditions of Tietê river basin. The models' ability to reproduce streamflow, sediment and nutrient loads at each monitoring station was measured by three indicators computed from the result's deviations from observed measurements.

The main novelty of this research is the comparison of a complex distributed watershed model (SWAT) with a more parsimonious hydrological model. We are particularly interested in understanding under which conditions the use of each model is to be recommended, namely when does the addition effort required to run the SWAT model leads to effective better results. The calibration of both models was performed jointly for the two case studies with the goal of obtaining consistent parameters values that lead to acceptable results in both river basins. The parameters that are common to both models' formulations were set to the same values to encourage the robustness and consistency of the model results.

This paper is organized as follows. Section 2 describes the mathematical formulation of both models, as well as the model's calibration and validation procedures. Section 3 describes the case studies and the available data. The research results are discussed in section 4 and the conclusions are offered in Section 5.

2. Methodology

2.1. Models description

2.1.1. SWAT model

SWAT is a continuous simulation model with a daily time step that includes components to simulate weather, hydrology, sediment, soil, crop, nutrients, pesticides, agricultural management, channel routing and reservoir routing. The watershed is partitioned into sub basins, each one being further subdivided into hydrologic response units (HRUs) that have a unique land cover, soil, slope and management practice combination. Each sub-basin contains at least one hydrologic response unit (HRU) and one main channel. The outputs of all HRU within each sub-basin are the water and mass inflow into the river network at the sub-basin outlet (Neitsch et al., 2009). This study used the SWAT2012 released on 2018.

Arnold et al. (2012) and Neitsch et al. (2011) provide a detailed description of SWAT. The computation of water flow through the watershed includes the land phase and the routing phase of the hydrologic cycle. The first phase computes the amount of water, sediment, nutrients and pesticides reaching the main channel in each sub basin, while the second phase traces the movement of water, sediments and reaching contaminants through the channel network to the outlet of the watershed (Neitsch et al., 2009).

The Soil Conservation Service method (SCS-CN) is the default of the model for estimating runoff and was used in this study. SWAT provides two methods for estimating the SCS retention parameter and the so-called "alternative method" was selected, which allows this parameter to vary with plant evapotranspiration. According to Neitsch et al. (2009), this alternative method was added because the traditional method may predict too much runoff, which was the case in our preliminary runs.

The soil profile is divided into 3 zones. The vadose zone and the shallow aquifer contribute to the stream flow, while the deep aquifer receives deep percolation from the shallow aquifer but does not contribute to the flow at the watershed outlet. The vadose zone is subdivided in soil layers, with the number of the layers depending on the soil types that occur in the area.

The Modified Universal Soil Loss Equation (MUSLE) (Williams, 1975) is used to estimate erosion and sediment yield from each HRU. The sediment yield carried by superficial flow on a given day can be calculated by:

$$SY_t = 11.8 \bullet (H_t \bullet T_t^{peak} \bullet A_{hru})^{0.56} \bullet K_s \bullet C \bullet P \bullet L \bullet S \bullet CFRG \quad (1)$$

where SY_t is the sediment yield carried by superficial flow on a given day (ton), H_t is the daily surface runoff volume (mm), T_t^{peak} is the peak runoff rate (m3/s), A_{hru} is the area of the HRU (ha), K_s is the USLE/MUSLE soil erodibility, C is the USLE/MUSLE cover and management factor, P is the USLE/MUSLE support practice factor, LS is the USLE/MUSLE topographic factor and $CFRG$ is the coarse fragment factor. The $CFRG$ can be calculated by:

$$CFRG = exp(-0.053 \bullet rock) \quad (2)$$

where $rock$ is the percentage of soil particles with a diameter larger than 2 mm in the first soil layer (%). The total sediment load reaching the stream, ST_t, is the sum of the sediments transported by superficial runoff, S_t^S, and by lateral and ground flow, S_t^{LG}:

$$ST_t = S_t^S + S_t^{LG} \quad (3)$$

In SWAT model the sediment transported by superficial runoff, S_t^S, is computed from total sediment yield from the watershed, SY_t, assuming that part is temporarily retained in the watershed by vegetation or in ponds. A lag is applied to:

$$S_t^S = (SY_t + SY_{t-1}) \bullet \left(1 - exp\left[-surlag / T^{conc} \right]\right) \quad (4)$$

where S_t^S is the sediment reaching the channel in day t (ton), and SY_t and SY_{t-1} are the amounts of sediment load generated in the

HRU on days t and t-1 (ton). The expression $\left(1 - exp\left[{}^{-surlag}/_{T^{conc}}\right]\right)$ in Eq. (4) represents the fraction of the total available sediment allowed to enter the reach on any one day. T^{conc} is the HRU time of concentration (hrs) and *surlag* is the surface runoff lag coefficient.

In large subbasins with a time of concentration greater than 1 day, only a portion of the surface runoff will reach the main channel on the day it is generated. SWAT incorporates a surface runoff storage feature to lag a portion of the surface runoff release to the main channel (Neitsch et al., 2002).

SWAT assumes that lateral and groundwater flow transport sediment to the main channel and estimates this load by:

$$S_t^{LG} = \frac{(L_t + G_t) \bullet A_{hru} \bullet SC}{1000} \tag{5}$$

where S_t^{LG} is the sediment loading in lateral and groundwater flow (ton), L_t is the lateral flow for a given day (mm), G_t is the groundwater flow for a given day (mm), A_{hru} is the area of the HRU (km^2), and SC is the concentration of sediment in lateral and groundwater concentration specified by the user (mg/L).

The sediment reaching the channel is routed, considering deposition and erosion as a function of the sediment load and flow transport capacity. The model computed the sediment transport capacity using a modification of Bagnold's equation (Bagnold, 1977).

SWAT considers two inorganic forms of nitrogen (nitrate (NO3-) and ammonia nitrogen (NH4+)) and three organic forms of nitrogen (active, stable and fresh organic N), as well as three organic forms of phosphorus (active, stable and fresh organic P), and three inorganic forms of phosphorus (stable, active and solution mineral P).

Ammonia and nitrate are associated with fertilizer usage, the stable and active organic P pools are associated with the soil humus, and fresh organic P is associated with crop residue and microbial biomass (Neitsch et al., 2005).

2.1.2. GWLF model

GWLF assumes a daily time step and uses the Soil Conservation Service method, based on the curve number concept, (SCS-CN) to estimate runoff, H_t, groundwater flow, G_t, and the total flow in the downstream section of the hydrographic basin, T_t. Calculation process were presented in Santos et al., 2018. The sediment yield is computed by the Universal Soil Loss Equation (USLE, Wischmeier and Smith, 1978) and nitrogen and phosphorus loads are estimated from average nutrient concentrations based on land use.

The GWLF model assumes that contaminants are transported in solid or dissolved phase with the solid phase contaminants coming from rural and urban areas and the dissolved contaminants coming from point sources, rural areas and groundwater. As such, all contaminant loads from point sources and groundwater are only in dissolved phase, and the contaminant loads from urban sources are only in solid phase.

Sediment yield, ST_t, is calculated by considering, separately, the soil loss and its subsequent transport through the runoff (Haith et al., 1992). The mean soil loss due to water erosion per unit area and time, t, (ton/ha/day), PS_t, can be estimated by the USLE.

$$PS_t = R_t \bullet K_s \bullet L \bullet S \bullet C \bullet P \tag{6}$$

where R_t is the rainfall erosivity factor (MJ.mm/h/ha) in time interval t; K_s is the soil erodibility factor of soil types (ton/MJ/mm), L is the topographic factor that expresses the length of the slope (km), S is the topographic factor that expresses the slope of the terrain or the degree (dimensionless), C is the factor that expresses the use and management of the soil and culture (dimensionless) and P is the factor that represents the conservationist (dimensionless) practices.

The R factor was calculated from the equation developed by Lombardi and Moldenhauer (1980) for Campinas, São Paulo, Brazil. Based on 22 years of rainfall records, a high correlation was found between measured soil erosion data and an erosion index, computed from the rainfall record. Based on a proposition from Fournier (1960), the erosion index is estimated from the following equation:

$$E_m = 68.730\left(\frac{\bar{P}_t^{m2}}{P_t^y}\right)^{0.841} \tag{7}$$

where E_m is defined as the monthly average erosion index (MJ.mm/h/year); $\bar{P}_t^m$ is the average monthly precipitation (mm) e P_t^y is the average annual precipitation (mm).

According to Lombardi and Moldenhauer (1980), the annual erosivity factor, R, is the sum of the erosion index monthly values. For this study, the equation was adapted to enable the calculation of R with a daily time step:

$$R_t = \left(\frac{P_t^{d2}}{\sum_{t \in m} P_t^{d2}}\right) \bullet E_m \tag{8}$$

where, P_t^d is defined as the daily precipitation (mm).

Sediment yield, ST_t (ton), is the product of soil loss and sediment delivery rate (SDR).

$$ST_t = PS_t \bullet SDR \tag{9}$$

SDR is the ratio between the sediment yield reaching a given river cross-section and the sediment production from erosive processes occurring in the watershed upstream of the cross-section. Vanoni (1975) proposed the following equation for the estimation of SDR.

$$SRD = 0.42 \bullet A^{-0.125} \tag{10}$$

where A is the drainage area of the river basin, in square miles.

The total of sediment yield, ST_t^{Total} (ton), was improved by the authors for implement the sediment yield product by the basin in the day before, according to the Eq. 11.

$$ST_t^{Total} = PS_t \bullet SDR + (1 - SRD) \bullet ST_{t-1} \tag{11}$$

The total nitrogen (N) and phosphorus (P) load can be calculated according to the following formulations:

$$N_t^D = N_t^{DP} + N_t^{DR} + N_t^{DG} \; P_t^D = P_t^{DP} + P_t^{DR} + P_t^{DG} \tag{12}$$

$$N_t^S = N_t^{SR} + N_t^{SU} \; P_t^S = P_t^{SR} + P_t^{SU} \tag{13}$$

where N_t^D and N_t^S are, respectively, the dissolved and solid phase nitrogen loads, and P_t^D and P_t^S are the dissolved and solid phase phosphorus loads. The exponents *DP*, *DR* and *DG* are relative to the loads of dissolved contaminants from point sources, rural areas and groundwater, respectively, and *SR* and *SU* relate to the solid phase contaminant loads from rural areas and urban areas, respectively. Next, the equations presented for the calculation of the nitrogen loads are applied in the same way for the calculation of the phosphorus loads.

The load of contaminants from point sources, N_t^{DP} (mg), can be calculated according to Eq. 14.

$$N_t^{DP} = \frac{s^{pop} \bullet Pop \bullet NC^{DP} \bullet (1 - r1^N) + (1 - s^{pop}) \bullet Pop \bullet NC^{DP} \bullet (1 - r2^N)}{T_t} \tag{14}$$

where *Pop* is the estimated population of the study area (hab), S^{pop} is the percentage of the population that has sewage treatment system, NC^{DP} is the concentration of nitrogen in the effluent from point sources, $r1^N$ is the rate of nitrogen removal by the sewage treatment system and $r2^N$ is the rate of removal of nitrogen from areas without sewage treatment system.

According to ABNT (2011) the composition of sanitary sewage has an average of 6–112 g/hab/day of total nitrogen and 1–5 g/hab/day of total phosphorus.

The load of dissolved contaminants from the rural area, N_t^{DR} (mg), can be calculated from the following formulation:

$$N_t^{DR} = \sum_k NC_k^{DR} \bullet H_{kt} \bullet A_k \tag{15}$$

where NC_k^{DR} is the concentration of dissolved contaminants (mg/L) from rural areas depending on the land use, k, H_k is the surface runoff (mm) on day t, A_k is the area of land use k (m2).

The average concentrations of dissolved contaminants from rural areas were adapted from Haith et al. (1992) and Li et al. (2010) and are shown in Table 1.

The solid phase contaminant load from the rural area, N_t^{SR} (g), is calculated from the ST_t (ton) sediment yield and the mean sediment concentration NC_k^{SR} (mg/kg) dependent on the land use, k.

$$N_t^{SR} = N_t^{SR} \bullet ST_t \tag{16}$$

According to Li et al. (2010), the mean concentrations of solid-phase sediments from rural sources, NC_k^{SR} and PC_k^{SR}, are in the ranges of 500 to 900 mg/kg and 120 to 393 mg/kg for nitrogen and phosphorus concentrations, respectively.

The load of contaminants from solid-phase urban areas, N_t^{SU} (mg), is calculated from the following formulation:

$$N_t^{SU} = \sum w_{kt} \bullet A_k \bullet NC_k^{SU} \tag{17}$$

where W_{kt} is the first-order washing coefficient, A_k is the area (ha) for land use k, and NC_k^{SU} is the concentration of nitrogen in urban areas (kg/ha).

The washing coefficient expresses the relationship between the surface runoff from urban areas and the accumulation and washing of contaminants (Sartor and Boyd, 1972; Amy et al., 1974). This concept is used in the SWMM model (Huber and Dickinson, 1988) and the STORM model (Hydrologic Engineering Center, 1977) and can be estimated by:

$$W_{kt} = 1 - e^{-0,181 \bullet H_{kt}} \tag{18}$$

where H_{kt} is the surface runoff (mm) referring to land use k on day t.

The values of accumulation of contaminants in urban areas, NC_k^{SU} and PC_k^{SU}, were adopted from Haith et al. (1992). In areas with a medium to a high population density, the daily rate of accumulation of urban contaminants varies from 0.028 to 0.031 kg/ha for

Table 1
Dissolved contaminants in rural areas.

Land use	Nitrogen (mg/L) - NC_k^{DR}	Phosphorus (mg/L) - PC_k^{DR}
Agriculture	0.71 – 5.04	0.07 – 0.11
Forest	0.06 – 0.19	0.00 – 0.012
Pasture	0.00 – 3.00	0.00 – 0.25
Grasslands	0.00 – 1.80	0.00 – 0.30
Sugar cane	0.00 – 2.90	0.00 – 0.26

nitrogen and from 0.002 to 0.007 kg/ha for phosphorus.

The load of contaminants in groundwater, N_t^{DG} (mg), can be obtained by:

$$N_t^{DG} = NC^{DG} \bullet A \bullet G_t \tag{19}$$

where NC^{DG} is the concentration of contaminants in groundwater (mg/L), A is the river basin area (m^2), and G_t is the contribution of the groundwater flow (mm) to the river.

The concentrations of contaminants dissolved in groundwater, NC^{DG}, were determined from standard values in the groundwater available in Li et al. (2010). In this study, a range of 0.1 to 19 mg/L for nitrogen concentration and a range of 0.01 to 0.1 mg/L for phosphorus concentration in groundwater were considered.

In this study, the GWLF method was programmed within Microsoft Excel, using VBA programming language, to take advantage of MS Excel native flexibility and functionality to manage and analyse data and model results.

2.2. Model calibration and validation

The calibration and validation of both models was performed jointly for the two case studies with the goal of obtaining consistent parameters values that lead to acceptable results in both river basins. The parameters that were shared between both models were assigned the same values and the parameters measuring similar concepts were assigned compatible values to reflect their physical nature and their dependence on the watershed's characteristics. It is true that as the models have a different formulation, the consequences of assigning a particular value to a given parameter are different in each model. However, in our case that the option to assign similar values to the shared parameters did not significantly degrade the model's performance. A split sample test validated the results (Klemeš, 1986). The first 3 years (1987–1989) were used as a warmup period to minimize uncertain initial conditions. Two subsequent and independent periods were used for calibration (1990–2000 for Jacaré Guaçu river basin and 1990–2003 for Atibaia river basin) and for validation (2000–2009 for Jacaré Guaçu river basin and 2003–2015 for Atibaia river basin). To facilitate the comparison between the model results, the same dataset of daily precipitation and potential evapotranspiration were used in both models. For the lumped model, the average precipitation and evapotranspiration over the whole watershed were computed as weighted averages of the precipitation and evapotranspiration values of each sub basin, as assigned by SWAT.

The calibration considered the optimization of multiple objectives, namely deviations from different aspects of the flow hydrographs, sediment loads, and nutrients loads, all measured at multiple sites. The result of multi-objective optimization problem is a set of Pareto optimum solutions. In our case, since the calibration was done manually, decisions were made along the process to retain the best single parameter set that offers a good equilibrium of reaching the different objectives.

The calibration adopted a systematic procedure (Madsen, 2000), which first focused on reproducing precipitation partition and the overall water balance of each basin. It then proceeded to reproduce the records of high and low stream flows and their timing. Finally, the attention focused on the sediment load data and on the nitrogen and phosphorus data. The parameters that are common to both models formulations were set to the same values to encourage the robustness and consistency of the model results.

The calibration focused on the parameters which most affect the models' results. This set of parameters was identified based on literature review and, in the case of SWAT, also based on a sensitivity analysis executed prior to the calibration effort (Neitsch et al., 2001; Lenhart et al., 2002; Arnold et al., 2012; Bonumá et al., 2013; Strauch et al., 2013; Me et al., 2015; Malagó et al., 2017). This is an important step as the number of parameters in SWAT hinders the possibility of manually calibrating all parameters.

The sensitivity analysis was performed using the sequential uncertainty fitting method (SUFI2) offered by the SWAT-CUP program. For each model parameter, the SUFI2 method computes the range of values that brackets most measured data within the model results (Abbaspour et al., 2007). The parameters with the shortest range are the ones which the model results are most sensitive too.

The model's calibration for sediment yield, nitrogen and phosphorus loads was executed by changing the parameters associated with each soil type and land use, thus affecting pollutant loads and concentration in the whole watershed.

2.3. Indicators to evaluate the model's performance

To evaluate the model's performance in reproducing the historical stream flows and water quality records the following set of indicators was used.

The Nash and Sutcliffe efficiency (NSE) (Nash and Sutcliffe, 1970) computes the sum of the squared difference between the model results and historical data and normalizes the results with sum of the squared difference between the historical data and its average (Eq. 20).

$$NSE = 1 - \left(\frac{\sum (T_t^{obs} - T_t^{sim})^2}{\sum (T_t^{obs} - \overline{T}_t^{obs})^2} \right) \tag{20}$$

where T_t^{obs} is observed value, $\overline{T}_t^{obs}$ is average observed value, T_t^{sim} is computed value, $\overline{T}_t^{sim}$ is average computed value. The value of NSE ranges from $-\infty$ to 1.0, with the latter being the optimal value. Values between 0.5 and 1.0 are generally viewed as acceptable levels of performance, whereas negative indicate that the mean observed value is a better predictor than the computed value (Moriasi et al., 2007).

The percent bias (Pbias) measures the average difference between the computed and measured values over a specified period:

$$P_{BIAS} = \left(\frac{\sum T_t^{obs} - \sum T_t^{sim}}{\sum T_t^{obs}} \right). 100 \quad (21)$$

Values of Pbias close to 0% reveal a smaller deviation of the model results from the measured values, but higher values for Pbias are acceptable when the measured values accuracy is relatively poor.

The coefficient of determination, r^2, describes the proportion of the measured data variance that is explained by the model. The coefficient r^2 ranges from 0 to 1, with higher values indicating a good adjustment. As r^2 only quantifies the dispersion, a model which systematically overestimates or under estimations all the time will still result in good r2 values close to 1.0, even if all predictions were inexact (Krause et al., 2005).

$$r^2 = \frac{(\sum [T_t^{obs} - \overline{T}_t^{obs}][T_t^{sim} - \overline{T}_t^{sim}])^2}{\sum (T_t^{obs} - \overline{T}_t^{obs})^2 \sum (T_t^{sim} - \overline{T}_t^{sim})^2} \quad (22)$$

Moriasi et al. (2007) argued that the performance of a hydrological using a monthly time step can be considered satisfactory if NSE > 0.5 and r^2 > 0.5, but that shorter time steps lead to poorer performances. Several authors have decided to accept the SWAT calibration when NSE computed with daily flows is above values in the range of 0.15 to 0.3 (Benham et al., 2006; Coffey et al., 2004; Nejadhashemi et al., 2012), showing how difficult is to model the highly variable and non-linear hydrological processes at a daily time step, especially when measured values may have significant measurement gaps and errors.

3. Study cases

3.1. Watershed data

The case studies are two tributary basins from the Tietê river, one of the largest tributaries of the Paraná river basin and one of the main rivers of the state of São Paulo (Fig. 1). The first study area is the Jacaré-Guaçu river basin, upstream of Cruzes river confluence, with an area of 1934 km^2 and the second one is the Atibaia river basin, with an area of 2818 km^2 that covers municipalities from São Paulo and Minas Gerais states.

The Jacaré-Guaçu river basin has its sources in Serra de Itaqueri (São Carlos, São Paulo State, Brazil) and flows into the Ibitinga Reservoir. The altitude of the river basin ranges from 551 m at the outlet to 930 m in the southeast part of the basin. The annual average precipitation is 1470 mm, with most of the rain falling from October to March. The basin relief influences the rainfall spatial

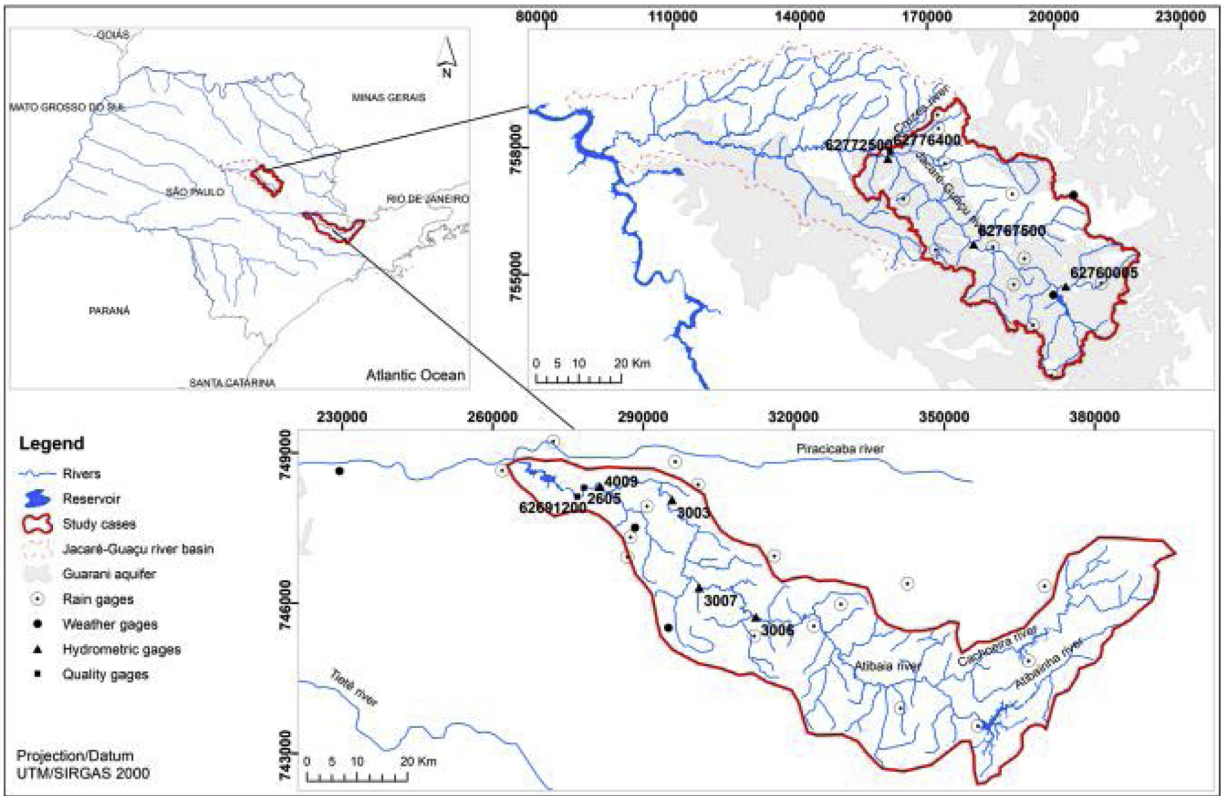

Fig. 1. Study area location with the rain, weather, hydrometric, quality gages.

distribution, with higher amounts of rainfall falling in the upper parts of the basin in the southeast. The Jacaré-Guaçu river basin spreads over the Guarani aquifer system (GAS), one of the world's largest aquifer and an important source of drinkable water for several cities, including Campo Grande, Ribeirão Preto, São José do Rio Preto and Araraquara, among others (Rabelo et al., 2004).

The Atibaia river basin spreads from its outlet at the junction of the Atibainha and Cachoeira rivers and to the sources of Cachoeira river in Minas Gerais state. The altitude ranges between 508 m to 1973 m at the outlet, in the west. A mountain range runs in the west and south of the river basin. The annual average precipitation is 1520 mm, with most of the rain falling from October to March.

Agriculture crops and mixed forests are the dominant land uses in both river basins because of a trend in the recent decades in the state of São Paulo that saw an intensification of the agricultural activity and the substitution of many crops by sugarcane and orange trees (Alkimim et al., 2015 and Strassburg et al., 2017).

Reforestation is also a significant activity in the Atibaia river valley, near its confluence with the Piracicaiba river, mainly due to the proximity of the paper and pulp industries located in the municipalities of Americana, Paulínia and Campinas (Comitê das Bacias Hidrográficas dos rios Piracicaba, Capivari e Jundiaí (CBH-PCJ, 2006).

3.2. Input data

A SWAT run requires a digital elevation model (DEM), as well as soil and land use digital maps. A 30 m resolution DEM, was obtained for both river basins from the SRTM (Shuttle Radar Topography Mission).

The soil types of both river basins were identified in a soil map produced by EMBRAPA (Empresa Brasileira de Pesquisa Agropecuária). The Jacaré-Guaçu river basin holds eight soil types, including red-yellow latosol (covering 55.4% of the river basin area), typic quartzipsamment (13.2%), typic eutrorthox (10.6%), typic haplortox (6.5%), typic paleudalf (5.1%), litololic soils (4.6%), hydromorphic soils (4.2%) and argiudoll (0.4%). The Atibaia river basin holds three main soil types, including red-yellow latosol (covering 61.0% of the river basin area), typic haplortox (37.8%), typic eutrorthox (1.2%).

The EMBRAPA map shows that red-yellow latosol, typic haplortox and typic eutrorthox soils cover 100% of the Atibaia river basin and 72% of Jacaré-Guaçu river basin. Red yellow soils are deep soils with a low clay content. Typic haplortox soils are several meters deep and are quite rich in clay and nutrients. Finally, typic euthorthox soils are weathered soils, highly permeable and with a variable clay content and low nutrients content. SWAT also requires data on 14 additional soil parameters, which were obtained from Freire et al (1978); Oliveira and Prado (1984); Lombardi Neto et al (1989), and Saxton and Rawls (2006).

A Landsat Thematic Mapper Satellite image from the second semester of 2001, with a spatial resolution of 30 × 30 m, was used to describe land use of Jacaré-Guaçu river basin. Seven types of land use were identified in the basin: agriculture (covering 35.66% of the river basin area), water (3.32%), range-grasses (3.63%), forest-mixed (5.02%), urban areas (13.57%), pasture (17.16%), and sugarcane (21.64%).

To describe the land use of the Atibaia river basin a map produced by the Water Resources Management Unit (UGRHI 5), based on a visual interpretation of a SPOT image from 2013, with 2.5 m spatial resolution, was used (UGRHI 5, 2013). Eight types of land use were identified in the basin: forest-mixed (covering 43.5% of the river basin area), mineral transportation (0.04%), sugarcane (1.4%), water (1.9%), range-grasses (3.0%), agriculture (3.8%), urban area (17.0%), and pasture (29.3%).

The meteorological and hydrological data for both river basins were obtained from the databases of two government agencies: ANA (Agência Nacional de Águas) and DAEE (Departamento de Águas e Energia do Estado de São Paulo).

In the Jacaré-Guaçu river basin, 10 rain gages, 3 hydrographs gages (62767500 – 568 km^2, 62760005 – 230.9 km^2 and 62772500 – 1135 km^2) and one water quality gage (62772500) were selected based on their location and record completeness (Fig. 1). Data on temperature data, humidity, wind speed and solar radiation was obtained from one gage operated by CRHEA (Centro de Recursos Hídricos e Ecologia Aplicada), located in the basin.

In the Atibaia river basin, 17 rain gages, 4 hydrograph gages (4009 – 2738km2, 3003 – 2490 km^2, 3006 – 1920 km^2 and 3007 – 2152 km^2) and 3 quality gages (62691200 and 2605) were selected based on their location and record completeness (Fig. 1). Data on temperature data, humidity, wind speed and solar radiation was obtained one weather gage operated by ESALQ (Escola Superior de Agricultura Luiz de Queiroz) located near to the basin.

Missing precipitation data were completed with the records from neighbour using multi-regression. The coefficient of determination, R2, of all regression equation was always greater than 0.6.

4. Results and discussion

A review of the relevant literature identified 17 parameters to which SWAT results are most sensitive (Table 2). To select among these the most important ones for flow prediction, two independent runs of SWAT-CUP were performed, one for each case study that led to the same 10 parameters, also highlighted in Table 2. The table groups the parameters by model component, namely groundwater flow, surface retention, river hydraulics, soil characteristics, as well as sediment and nutrients transport. For each parameter, the table indicates the expected range of values, the default value and the final value obtained after calibration (calibrated values).

The preliminary SWAT runs, using the parameters default values, lead to an overestimation of the observed stream flow record, particularly the high flow values. The calibration procedure thus proceeded to reduce these peak flows. Curve numbers (CN2) were reduced by 20% uniformly across the watershed to promote infiltration and base flow, at the expense of stormflow. Available water capacity of the topsoil layer (SOL_AWC) was also reduced by 50% to reduce the soil holding capacity, increase groundwater

Table 2
Calibrated parameters of SWAT model with their default and calibrated values.

		Parameters	Relevant according to SWAT CUP	Definition	Unit	Range	Default value	Calibrated value
Water	Ground water flow	GW_REVAP.gw		Groundwater "revap" coefficient	–	0.02 to 0.2	0.02	0.04
		REVAPMN.gw	✓	Threshold depth of water in the shallow aquifer required for "REVAP" or percolation to the deep aquifer to occur.	mm	0 to 1000	750	400
		GWQMN.gw	✓	Threshold depth of water in shallow aquifer required for the return flow to occur.	mm	0 to 5000	1000	500
		ALPHA_BF.gw		Baseflow alpha factor	days	0 to 1	0.048	0.001
		RCHRG_DP.gw	✓	Deep aquifer percolation fraction	mm	0 to 1	0.05	0.04
		GW_ DELAY.gw	✓	Groundwater delay	days	0 to 500	31	20
	Surface Retention	CANMX.hru	✓	Maximum canopy storage	mm	0 to 100	0	30
		ESCO.hru	✓	Soil evaporation compensation factor	–	0.01 to 1	0.95	0.4
	River hydraulic	CH_K2.rte	✓	Effective hydraulic conductivity in main channel alluvium	mm/hr	−0.01−0.01 to 500	0	3.2
		CH_K1.sub	✓	Effective hydraulic conductivity in the tributary channel alluvium	mm/hr	0 to 300	0	5
		CH_N1.sub		Manning's n value for the tributary channels	mm/hr	0.01 to 30	0.014	0.03
	Soil characteristics	SLSOIL.hru	✓	Slope length for lateral subsurface flow	m	0 to 150	0	40
		CNCOEF.bsn		Weighting coefficient for calculating retention dependent of plant evapotranspiration	–	0.5 to 2	2	1.6
		CN2.mgt		Initial SCS runoff curve number for moisture AMC-II	–	0 to100	Varies	0.8[b]
		SOL.awc	✓	Available water capacity of soil layer	mm/mm	0 to 1	Varies	0.5[b]
Sediment		USLE_P.mgt		USLE support practice factor	–	0 to 1	1	0.8
		SPCON.bsn		Coefficient in sediment transport equation	–	0.0001 to 0.01	0.0001	0.01
		CH_COV1.rte		Channel erodibility factor	–	−0.05 to 0.6	0	0.1
		CH_COV2.rte		Channel cover factor	–	−0.001 to 1	0	0.1
		LAT_SED.hru		Sediment concentration in lateral flow and groundwater flow	mg/L	0 to 5000	0	3000
Nitrogen		NPERCO.bsn		Nitrogen percolation coefficient	–	0 to 1	0.3	0.2
		SHALLST_N.gw		Nitrate concentration in the shallow aquifer	mg/L	0 to 1000	0	10
		CDN.bsn		Denitrification exponential rate Coefficient	–	0 to 3	1.4	0.3
		CMN.bsn		Rate factor for humus mineralization of active organic nitrogen	–	0.001 to 0.003	0.0003	0.002
		RSDCO.bsn		Residue decomposition coefficient	–	0.02 to 1	0.05	0.09
		N_UPDIs.bsn		Nitrogen uptake distribution factor	–	0 to 100	20	0.2
		RCN.bsn		Concentration of nitrogen in rainfall	mg/L	0 to 15	0	0.1
		HLIFE_NGW.gw		Half-life of nitrate–nitrogen in the shallow aquifer	days	0 to 200	0	190
		LAT_ORGN.gw		Organic N in the base flow	mg/L	0 to 200	0	0.055
		EROGN.hru		Organic N enrichment ratio	–	0 to 5	0	3
		CH_ONCO.rte		Organic nitrogen concentration in the channel	ppm	0 to 100	0	0.01
		BC1.swq		Rate constant for biological oxidation for NH4 to NO2 in the reach at 20 °C	1/day	0.1 to 1	0.55	1
		BC2.swq		Rate constant for biological oxidation for NO2 to NO3 in the reach at 20 °C	1/day	0.2 to 2	1.1	0.7
		BC3.swq		Rate constant for hydrolysis of organic N to NH4 in the reach at 20 °C	1/day	0.2 to 0.4	0.21	0.4
		RS3.swq		Benthic source rate for NH4-N in the reach at 20 °C	mg/m2	0 to 1	0.5	0.2

(*continued on next page*)

Table 2 (*continued*)

	Parameters	Relevant according to SWAT CUP	Definition	Unit	Range	Default value	Calibrated value
Phosphorus	SOL_ORG.chm		Initial organic P concentration in surface soil layer	mg/kg	0 to 100	0	10
	PPERCO.bsn		Phosphorus percolation coefficient	–	10 to 17.5	10	15
	PHOSKD.bsn		Phosphorus soil partitioning coefficient	–	100 to 200	175	100
	P-UPDIS.bsn		Phosphorus uptake distribution factor	–	0 to 100	20	0.1
	PSP		Phosphorus sorption coefficient	–	0.01 to 0.7	0.4	0.7
	LAT_ORGP.gw		Organic P in the base flow	mg/L	0 to 200	0	0.2
	BC4.swq		Rate constant for mineralization of organic P to dissolved P in the reach at 20 °C	1/day	0.01 to 0.7	0.35	0.5
	RS2.swq		Benthic source rate for dissolved phosphorus in the reach at 20 °C	mg/m2	0.001 to 0.1	0.05	0.08

[a]Varies with land use and soil type; [b]Multiplying factor to be apllied to the parameter original value.

percolation and to delay the flow reaching the river. The soil evaporation compensation factor (ESCO) was reduced to 0.4 to promote the evaporative demand from lower soil levels. The parameter GW REVAP, a coefficient reflecting the capability to move water from the shallow aquifer to the overlaying unsaturated soil zone, was set to 0.12, which indicates more water is available for baseflow discharge. The REVAPMN, defining the threshold depth of water in the shallow aquifer for return flow to the root zone to occur, was set to 300 mm.

Once the magnitude and the variability of base flow and hydrograph peaks were reproduced, the overall water balance was adjusted using the RCHRG_DP parameter. The value for RCHRG_DP was set to 0.04, which means that 4% of infiltrated water is lost to a deep aquifer. CANMX describing the storage capacity of a canopy to hold intercepted precipitation was set to 60. The value of CH_K1 e CH_K2 indicating the rate of water loss from streams to ground water was set to 5 mm/hr and 3.2 mm/hr, which assumes the presence of losing streams within the watersheds (Gitau and Chaubey, 2010).

According to Arnold et al. (2012), the threshold depth of water in shallow aquifer required for the return flow to occur (GWQMN) and the baseflow alpha factor (ALPHA_BF) are also important in calibration. At the beginning of calibration, the base flow was very low, so the GWQMN value was decreased from 1000 to 300 mm, to regulate the movement of water inside the aquifer. The variable ALPHA_BF affects the shape of the hydrograph, and it was necessary to decrease this parameter to 0.001. The groundwater delay time (GW_DELAY), which reflects the time lag that it takes water in the soil to enter the shallow aquifer, was decreased to 20 days.

The overall water balance for both river basins computed by both models is very similar and lead to an average annual outflow from the basin, within 5% of observed stream flow in most cross-sections. Water losses to deep aquifer are around 3% of precipitation.

The Manning's n parameter for the main channel (CH_N1) were set to 0.03 which are assigned to normal channels with clean structure full stage, no riffs or deep pools (Chow, 1959). Regarding the parameters related to soil characteristics, the slope length for lateral subsurface flow (SLSOIL), related to the interflow generation, was adjusted for 40 m. The weighing coefficient for calculating retention dependent of plant evapotranspiration (CNCOEF) was modified to 1.6.

Table 3 shows the default values of SCS-CN and GWLF models parameters suggested by the literature (Haith, Shoemaker 1987; Haith et al., 1992; Li et al., 2010; Niraula, 2013), based on watershed characteristics, as well as the values obtained following calibration. The lumped model parameters affecting streamflow are the curve number (CN), the river basin water storage capacity (U_{max}), the groundwater recession constant (α) and the deep recharge coefficient (β). These parameters were calibrated for each hydrometric station sub-basin, starting at the upstream hydrometric stations, moving to the intermediate stations and finally to the downstream station.

In both study cases, the CN values were reduced from the original value to increase infiltration. The river basins water storage capacities (U_{max}) were also reduced from default values to reduce evapotranspiration and increase infiltration. This need was also felt calibrating the corresponding parameters of SWAT, which are CN2 and SOL_AWC respectively. The groundwater recession constant (α) was set to lower values than the originals therefore reducing the response time to recharge. During SWAT calibration the corresponding parameter (ALPHA_BF) was also reduced from the default value.

Figs. 2 and 3 compare the daily and monthly measured stream flow at the downstream station of Jacaré-Guaçu river basin (62772500) with the computed flow by SWAT and GWLF models. Figs. 4 and 5 compare the daily and monthly measured stream flow at the downstream station of Atibaia river basin (upstream the reservoir) (4009), with the computed flow data. Table 4 and 5 shows the obtained values for each performance indicator and study cases. All figures and tables separate the calibration period (October/1991 to September/2003) from the validation period (October/2003 to October/2016).

The results show that both models can reproduce the daily flow variability for both study cases, although failing to replicate all values accurately, particularly some of largest daily flow measurements which are overestimated (Fig. 4). The GWLF model significantly overestimates the daily flow values at specific periods, namely in 1994/95, 1995/96, 2001/02 and 2002/03 at the Jacaré-Guaçu river basin. These streamflow values are the result of high precipitation values, which GWLF model formulation does not attenuated as much as the SWAT formulation.

The computed daily streamflow results show some fluctuation around the observed values which may be due the SCS methodology used in both models. It seems that in days of high precipitation, the daily precipitation excess is probably overestimated and is not distributed as flow throughout the following days.

When model results are aggregated at a monthly time step, the peak flows are reproduced with reasonable accuracy, with the GWLF model presenting a slightly better adjustment to the observed values than SWAT (Figs. 3 and 5). The observed fluctuation in daily values disappears as it is aggregated within each month.

The performance indicators (NSE, Pbias and r^2) values, presented in Table 4 and Table 5, corroborate these conclusions. The indicators show that the models' ability, and particularly GWLF, to reproduce streamflow at a daily time step is poor at all monitoring stations of Jacaré-Guaçu river basin and near to satisfactory in most monitoring stations of the Atibaia river basin. The values obtained with daily streamflow are low but not unusual, as the results from Benham et al. (2006) and Coffey et al. (2004) show. As expected, the values obtained for the calibration periods are usually better than the values obtained for the validation period.

At a monthly timestep, both models have a reasonable performance, with NSE ranging from 0.42 to 0.89, and continue to perform better at the Atibaia river basin than at Jacaré-Guaçu river basin.

The worse model performance in reproducing streamflow at Jacaré-Guaçu river basin may be due to difficulties of simulating surface water - groundwater interactions, as this basin spreads over the Guarani aquifer system. The poor model performance may also be due to the poor quality of monitoring data, namely precipitation and streamflow, as some authors have already pointed out (e.g. (Monteiro, 2016; Pontes et al., 2016). In particular, the model performance is strongly conditioned by precipitation estimates, and thus by precipitation data availability and monitoring stations location. The precipitation records of Jacaré-Guaçu river basin show 13.18% of missing data against 3.04% of missing data in the precipitation records of Atibaia river basin. And whereas the rain

Table 3
Calibrated parameters of GWLF model with their default and calibrated values.

	Parameter	Definition	Unit	Default value		Calibrated Value	
				Hydrometric gages			
				Jacaré Guaçu	Atibaia	Jacaré Guaçu	Atibaia
Water	CN	Curve number	–	69/72/76[a]	65/63/60/60[b]	45/65/42[a]	60/50/55/45[b]
	$U_{máx}$	Field capacity	mm	105	105	20/70/30[a]	85/80/80/85[b]
	Alfa (α)	Groundwater recession constant	–	0.006	0.005	0.002	0.004
	Beta (β)	Deep recharge coefficient	–	0.0	0.0	0.0003/0.0008/0.0002[a]	0.004
				Quality gages			
				62772500		**2605**	62691200
Sediment	K	Soil erodibility factor	ton/h/MJ.mm	0.03		0.03	0.025
	LS	Topographic factor	–	0.10		0.26	0.86
	P	USLE equation suport practices	–	0.60		0.80	
	C	Factor of conservation practices	–	0.30		0.90	
	SDR	Sediment Delivery Ratio	–	0.062		0.009	0.056
Nitrogen and phosporus	NC^{DP}	Dissolved nitrogen in point sources	g/hab/day	6.00 – 112.00		7.00	6.00
	$r1^{N}$	Nitrogen and Phosphorus removal rate by sewage treatment system	–	0.80		0.70	0.80
	$r2^{N'}$	Rate of nitrogen and phosphorus removal from areas without sewage treatment	–	0.30		0.20	
	NC_k^{DR}	Dissolved nitrogen in rural sediments	mg/L	0 – 2.90		0.02 – 0.1	
	NC_k^{SR}	Solid nitrogen in rural sediments	mg/kg	500 – 900		700.00	500
	NC_k^{SU}	Solid nitrogen in urban sediments	k/ha	0.028 - 0.031		0.030	0.0030
	NC^{DG}	Nitrogen in groundwater	mg/L	0.10 – 19.00		0.50	
	s^{pop}	Percentage of population having sewage treatment system	–	0.70		0.80	1
	CN	Pasture	–	47.80		47.55	
		Forest-mixed	–	69.30		50.00	69.35
		Urban area	–	98.00		98.00	98.00
		Range-grasses	–	58.30		58.30	58.30
		Agriculture	–	72.90		60.00	72.86
		Sugarcane	–	69.20		62.00	69.15
	PC^{DP}	Dissolved phosphorus in point sources	g/hab/day	1.00 – 5.00		5.00	
	PC_k^{DR}	Dissolved phosphorus in rural sediments	mg/L	0 – 0.30		0.09 – 0.50	
	PC_k^{SR}	Solid phosphorus in rural sediments	mg/kg	120 - 393		500.00	
	PC_k^{SU}	Solid phosphorus in urban sediments	k/ha	0.002 - 0.007		0.003	0.0025
	PC^{DG}	Phosphorus in groundwater	mg/L	0.01 – 1		0.7	0.2

This parameters values corresponding to different hydrometric gages related to Jacaré-Guaçu and Atibaia river basin respectively: [a]62760005, 62767500, 62772500 and [b] 3006, 3007, 3003 and 4009.

gages density in both basins is similar (1.06 gages per 100 km^2 in Jacaré-Guaçu river basin and 0.51 gages per 100 km^2 in Atibaia river basin), some smaller watersheds are not well covered by the precipitation monitoring network. A good example of this challenge is the river basin of the Jacaré-Guaçu upstream station (62760005), which spreads over a mountainous region and is monitored by a single precipitation station.

The best model' performance is obtained at the downstream stations of both river basins (62772500 and 4009), where NSE are always above 0.55 even for the validation period. The model's better performance at the downstream stations indicates that the aggregating effect arising from larger watersheds facilitates the model's calibration. Existing deficiencies in estimating flow at a local scale due to weak monitoring or poor representation of the watershed characteristics do not have a significant impact at a larger scale. A similar aggregating effect also explain why the models results aggregated at a monthly time step compare better with observed values, than when this comparison is performed at a daily time step. Both models and GWLF, in particular, have difficulty in reproducing the flow variability at shorter time periods.

Overall, the results show that although SWAT has a better performance in reproducing the daily flow values, this comparative advantage is not evident at a monthly time step.

To reproduce sediment yield with SWAT, the USLE equation support practices parameters (USLE_P) was identified as the most important one and was set to 0.8 in both study cases, which indicates the existence of conservation practices in the basin what is actually found in the field. The coefficient in the sediment transport equation (SPCON) calibrated was set to 0.01 which indicates a larger amount of sediment entering the channel. The channel erodibility factor (CH_COV1) and the channel coverage factor (CH_COV2) are factors that also influence the transport of sediments in the channel, since they determine the channel susceptibility to

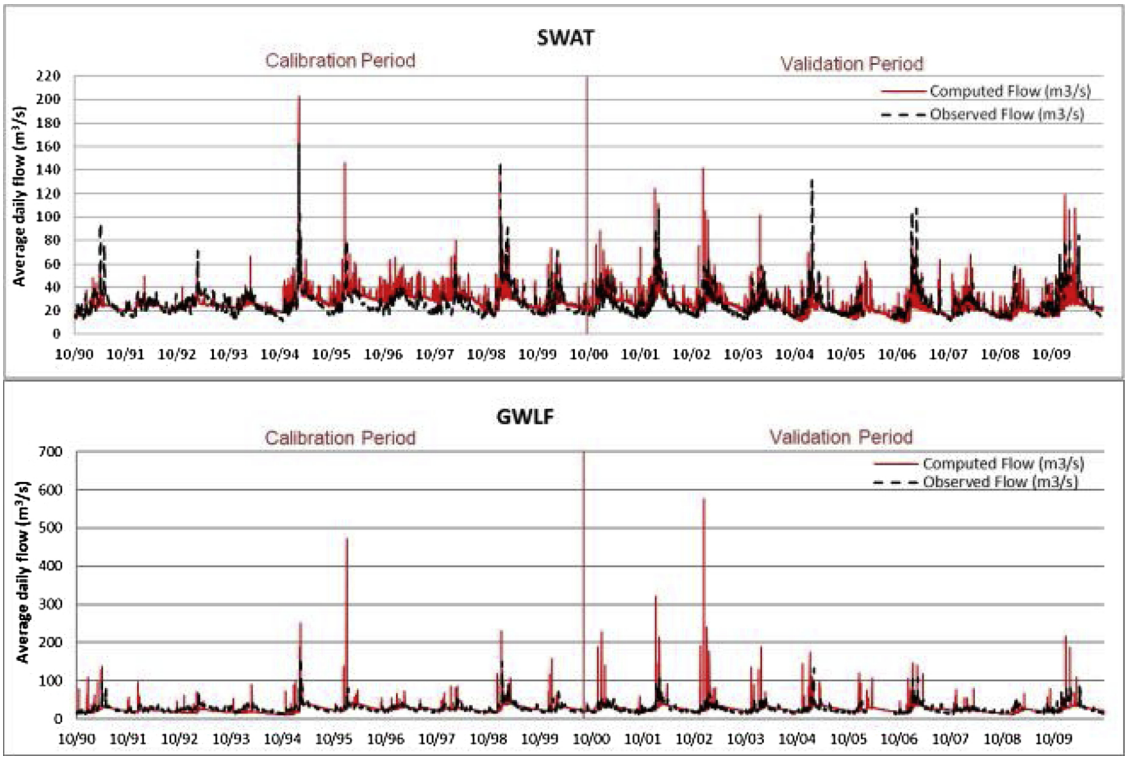

Fig. 2. Comparison of SWAT and GWLF computed daily flows with the observed flow at station 62772500 (Jacaré-Guaçu river basin).

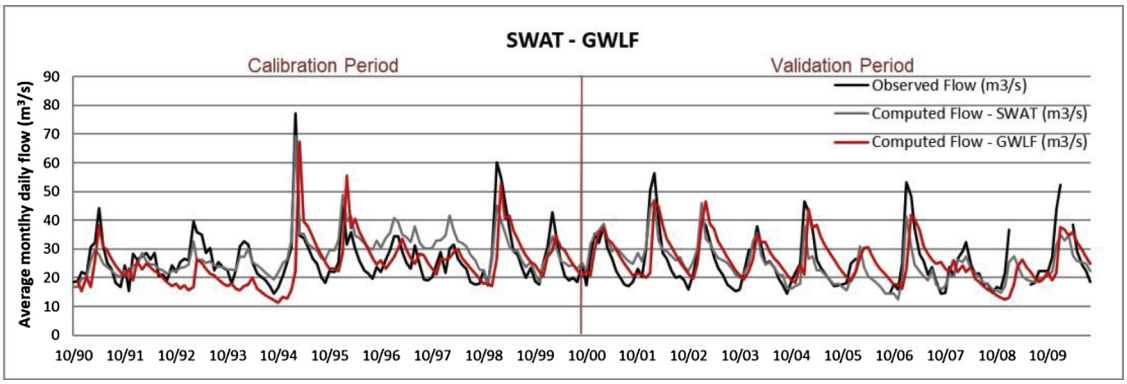

Fig. 3. Comparison of SWAT and GWLF computed monthly flows with the observed flow at station 62772500 (Jacaré-Guaçu river basin).

erosion and the channel protection to erosion. Both parameters were set to 0.1 indicating a low susceptibility to channel erosion.

In SWAT, the nitrogen loads are mostly sensitive to the nitrogen percolation coefficient (NPERCO) and to the nitrate concentration in the shallow aquifer (SHALLST_N), while the phosphorus loads are sensitive to the initial organic P concentration in soil layer (SOL_ORGP), to the phosphorus percolation coefficient (PPERCO) and to the phosphorus soil-partitioning coefficient (PHOSKD). In GWLF, the most relevant parameters are related to the dissolved contaminants in rural areas (NC_k^{DR} and PC_k^{DR}).

The computed values of sediment yield, total nitrogen and phosphorus loads were compared with bi-monthly measurements performed at Jacaré-Guaçu quality station (62776400), from January/2001 to December/2010, and at Atibaia quality stations (2605 and 62691200), from January/2009 to December/2016. The comparison between the models results and the observed values is hindered due to the bimonthly sampling interval of the latter values.

Table 6 shows the computed performance indicators for both models and for both cases studies. Figs. 6, 7 and 8 compare the sediment yield values. SWAT sediment yield estimates present a higher variability than the GWLF estimates, at times exceeding the observed peak values. The GWLF model generates a smoother time series of results that underestimate both the observed values and the SWAT estimates during recession periods. This is mostly because GWLF applies the USLE equation with rainfall intensity representing the erosive factor, while SWAT resorts to the MUSLE equation, using runoff volume and peak flow rate to compute the sediment yield. The smoother variability of streamflow, when compared to precipitation, resulting from surface runoff storage that

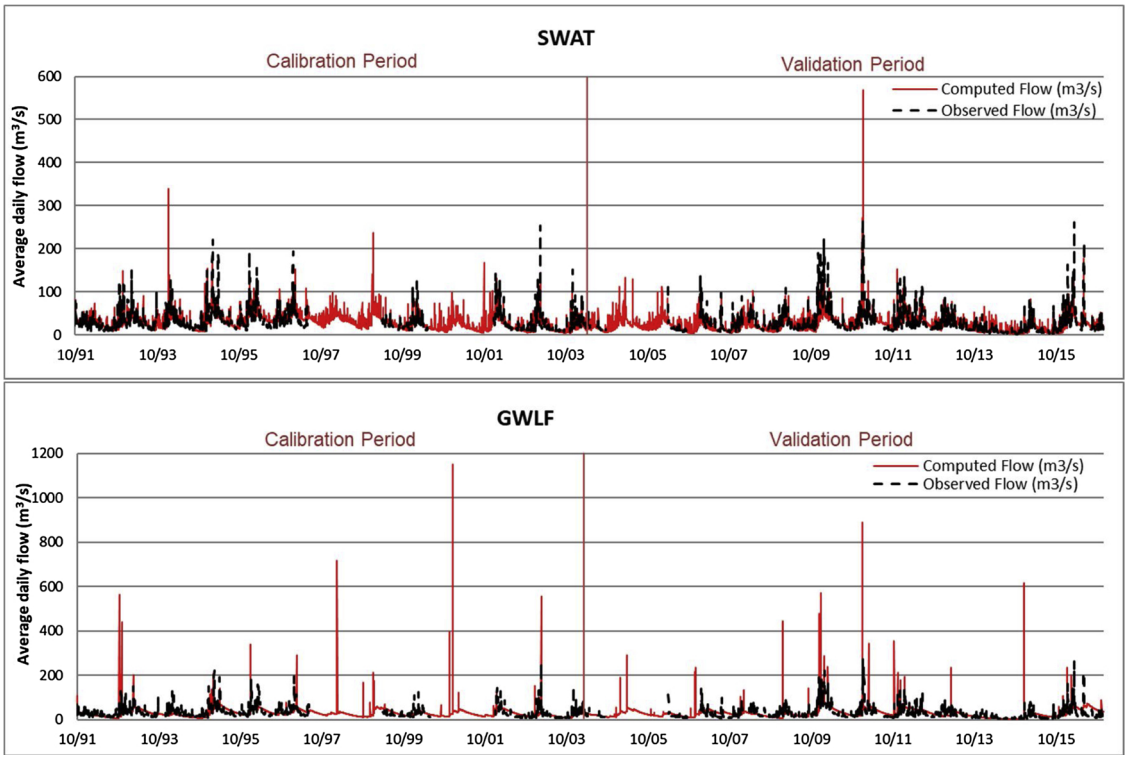

Fig. 4. Comparison of SWAT and GWLF computed daily flows with the observed flow at station 4009 (Atibaia river basin).

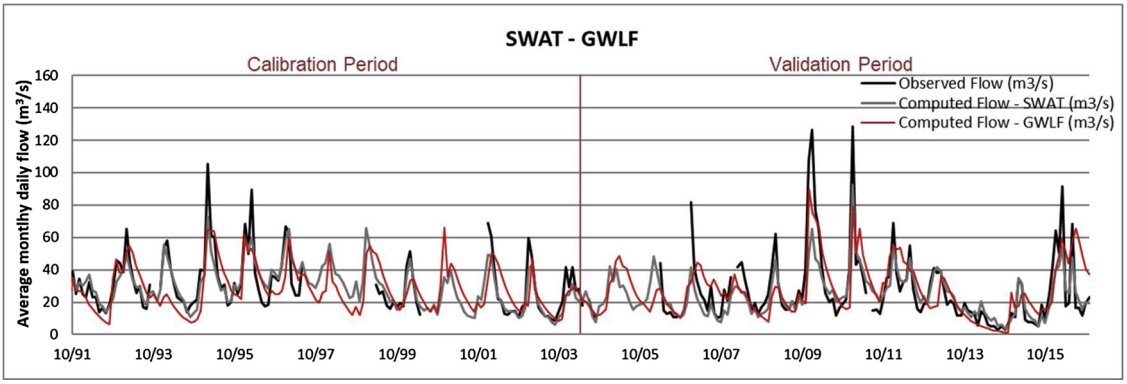

Fig. 5. Comparison of SWAT and GWLF computed monthly flows with the observed flow at station 4009 (Atibaia river basin).

Table 4
SWAT and GWLF models performance in reproducing daily and monthly streamflow for Jacaré-Guaçu river basin.

	Calibration - SWAT			Validation - SWAT			Calibration - GWLF			Validation - GWLF		
Gage	NSE	Pbias	r^2	NSE	Pbias	r^2	NSE	Pbias	r^2	NSE	Pbias	r^2
	Daily											
62760005	0.15	−1.31	0.09	−0.03	1.38	0.15	−0.66	2.16	0.09	−0.57	−6.85	0.11
62767500	0.21	−3.30	0.29	−0.74	−10.88	0.24	0.18	21.82	0.34	−0.84	0.95	0.23
62772500	0.27	−6.77	0.38	0.49	3.15	0.32	−0.64	3.24	0.24	−0.59	−3.95	0.13
	Monthly											
62760005	0.30	−1.75	0.15	0.35	10.30	0.21	0.34	2.28	0.24	0.68	−6.76	0.36
62767500	0.32	−4.84	0.31	0.68	−10.83	0.73	0.31	20.88	0.56	0.66	0.45	0.71
62772500	0.55	−6.65	0.59	0.81	3.21	0.65	0.59	5.70	0.64	0.84	−2.65	0.69

Table 5
SWAT and GWLF models performance in reproducing daily and monthly streamflow for Atibaia river basin.

Gage	Calibration - SWAT			Validation – SWAT			Calibration - GWLF			Validation - GWLF		
	NSE	Pbias	r^2	NSE	Pbias	r^2	NSE	Pbias	r^2	NSE	Pbias	r^2
	Daily											
3006	0.58	0.45	0.41	0.30	−12.89	0.39	0.23	−13.05	0.29	0.23	8.64	0.24
3007	0.31	12.53	0.41	0.32	−3.56	0.44	0.21	−6.50	0.24	0.21	−6.50	0.24
3003	0.70	−7.86	0.49	0.50	−8.98	0.50	0.52	−0.48	0.26	0.30	−8.09	0.27
4009	0.77	−21.85	0.62	0.61	−7.32	0.53	0.50	2.49	0.34	0.16	−0.94	0.27
	Monthly											
3006	0.86	0.44	0.71	0.62	−11.80	0.64	0.70	17.26	0.47	0.42	10.40	0.44
3007	0.81	12.81	0.88	0.70	−8.67	0.72	0.71	−7.74	0.43	0.53	−9.36	0.57
3003	0.88	−6.93	0.76	0.70	−7.25	0.72	0.76	0.73	0.47	0.60	−8.21	0.55
4009	0.95	−4.89	0.88	0.77	−4.67	0.72	0.86	2.60	0.70	0.76	−1.09	0.70

Table 6
SWAT and GWLF models performance in reproducing water quality for Jacaré-Guaçu and Atibaia quality station.

Model/Station		Sediment yield			Total Nitrogen load			Total Phosphorus load		
		NSE	Pbias	r2	NSE	Pbias	r2	NSE	Pbias	r2
Jacaré-Guaçu River basin										
62776400	**SWAT**	0.23	9.02	0.06	−9.20	−483.54	0	0.23	14.72	0.19
	GWLF	0	−5.86	0.11	0	26.99	0	−0.52	6.39	0
Atibaia River Basin										
2605	**SWAT**	−0.04	39.50	0.07	−1.12	76.04	0	−0.18	20.00	0.20
	GWLF	0.41	34.59	0.50	−0.28	43.93	0	−0.25	72.10	0
62691200	**SWAT**	−0.04	33.33	0.04	−1.34	76.62	0	−0.04	18.44	0.35
	GWLF	0.40	−20.40	0.47	0	−10.26	0.19	−0.24	65.35	0.11

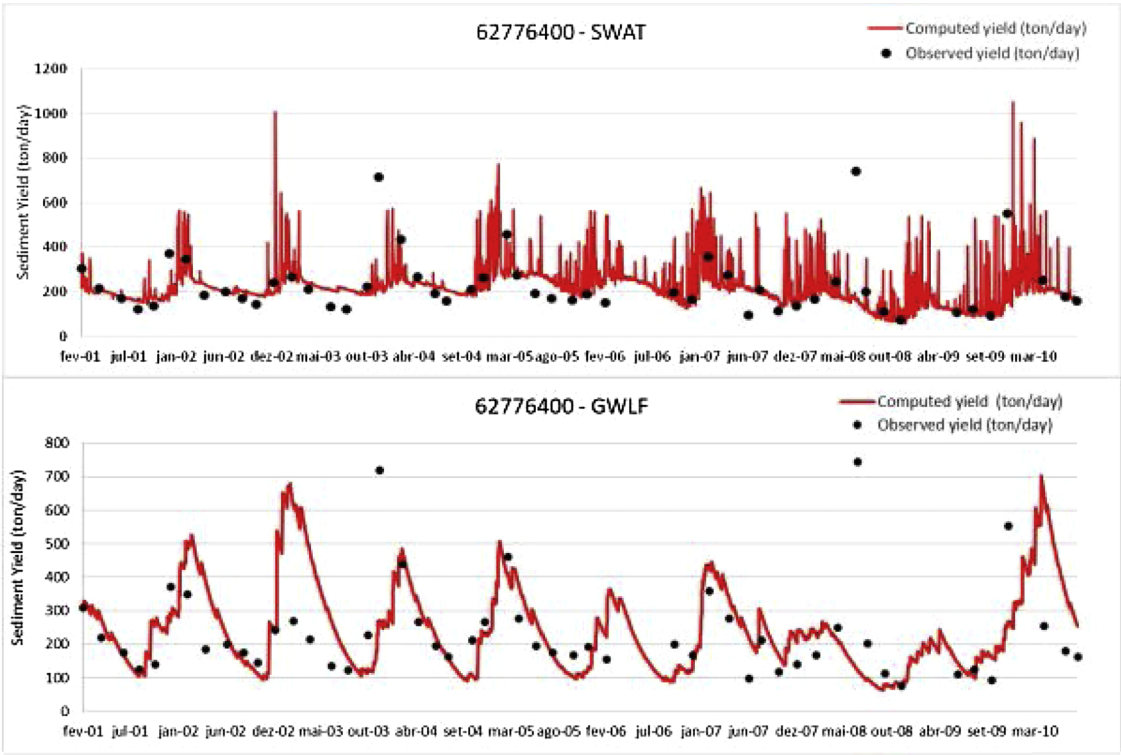

Fig. 6. Performance of SWAT and GWLF models for sediment yield at station 62776400 (Jacaré-Guaçu river basin).

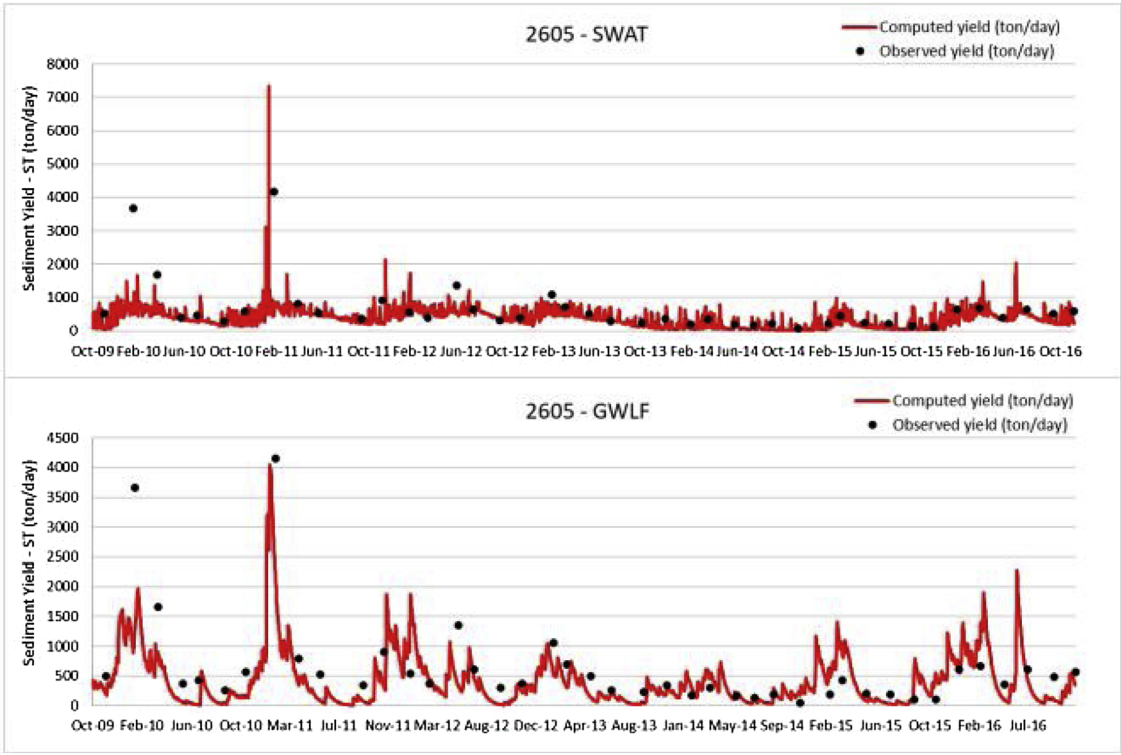

Fig. 7. Performance of SWAT and GWLF models for sediment yield at station 2605 (Atibaia river basin).

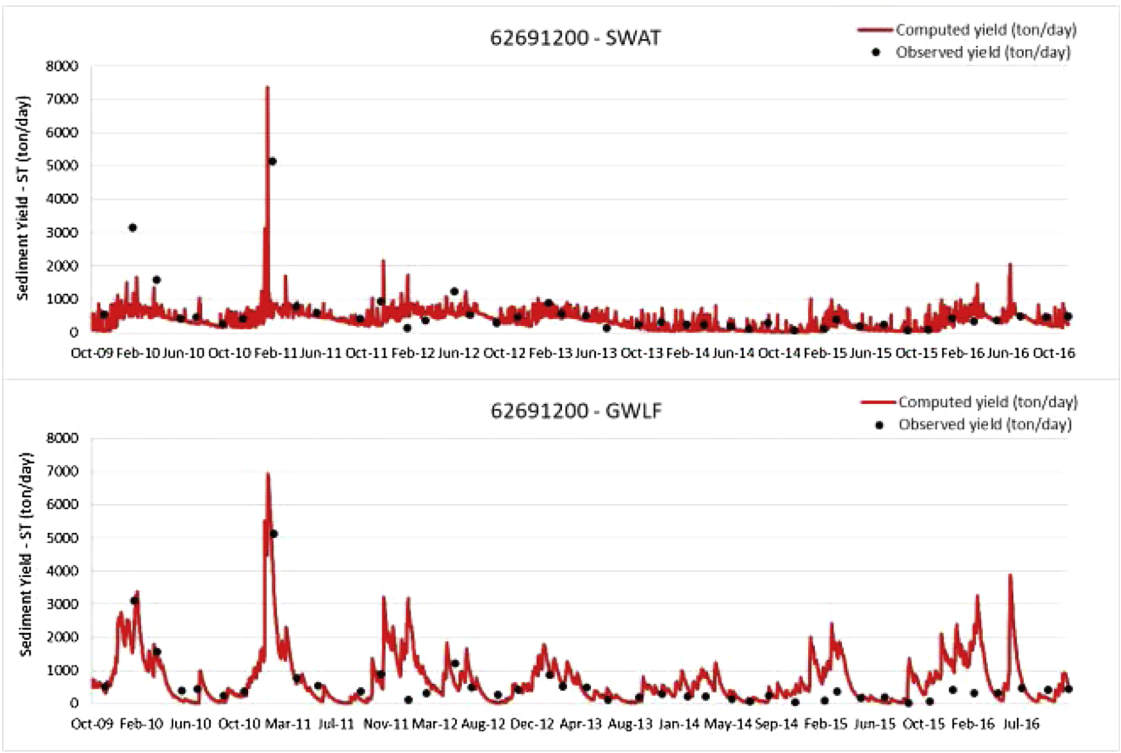

Fig. 8. Performance of SWAT and GWLF models for sediment yield at station 62691200 (Atibaia river basin).

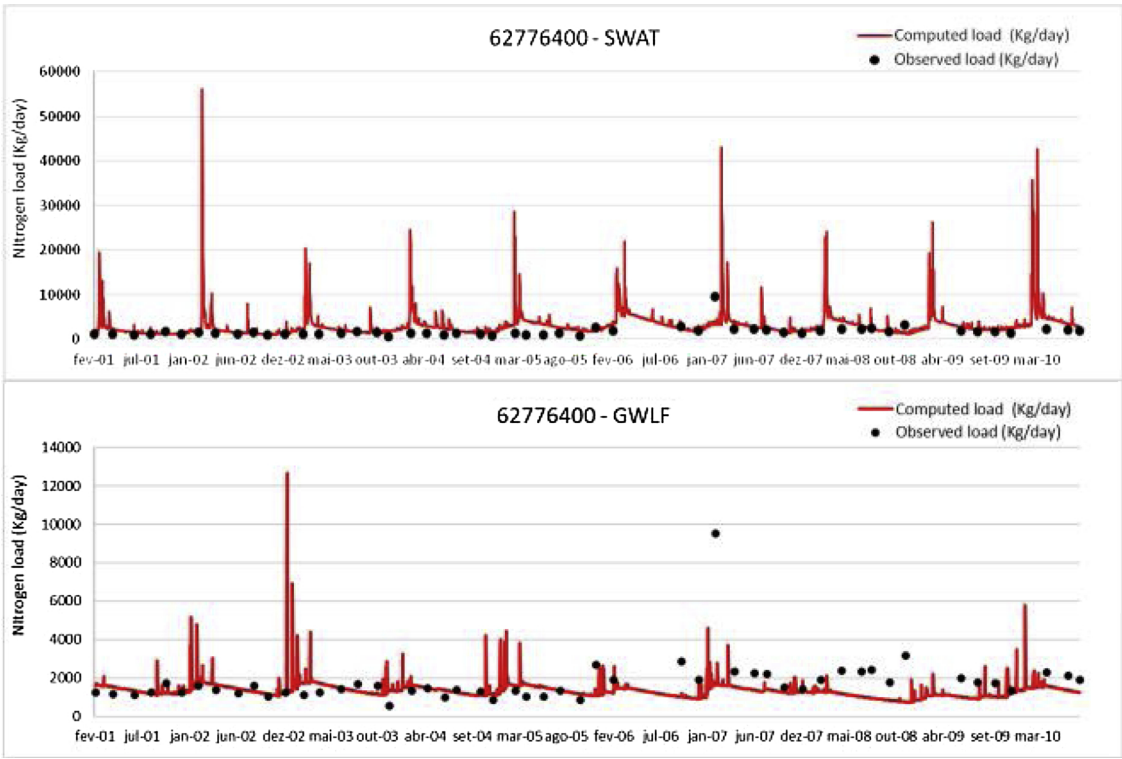

Fig. 9. Performance of SWAT and GWLF models for total nitrogen load at station 62776400 (Jacaré-Guaçu river basin).

lags precipitation and runoff release to the main channel, dampens the sediment variability. SWAT also uses sediment transport equations to simulate erosion and deposition along the main channel.

From the figures, both models are able to reproduce the order of magnitude and the major variations of the sediment yield, although not with accuracy. Table 6 shows that GWLF leads to better sediment yield estimates, especially in the Atibaia river basin computed values, where NSE and r2 reach values close to 0.5.

Figs. 9, 10 and 11 compare the total nitrogen load values computed for and measured at the three monitoring stations. Both models can reproduce the order of magnitude of the observed values during low flows but offer highly variable estimates that significantly exceed the by-monthly observed values. The performance indicators values (Table 6) confirm this poor performance, with the GWLF model showing slightly better results.

Figs. 12, 13 and 14 compare the total phosphorus load values computed for and measured at the three monitoring stations. The results of both models for the station located in the Jacaré-Guaçu river basin presented a good fit for the low observed values but fail to predict the peaks (Fig. 12). SWAT modelled peak values present a delay when compared with the GWLF estimates, due to the runoff lag equation used by the SWAT. The performance indicators suggest that SWAT performs slightly better than GWLF. Overall, the phosphorus estimates from both models, but particularly from SWAT, are better than the nitrogen estimates.

The difficulties in reproducing nutrients loads and sediment transport also arise from the accumulation of estimation errors all through the computing sequence, from stream flow to sediment transport and, finally, to nutrients loads.

5. Conclusions

The research showed the difficulty hydrological models have to reproduce daily flows from meteorological daily data in real-case situations, where the existing precipitation dataset is limited and is not able to fully represent the time and space variability of this variable. When the models' results are aggregated at monthly time step to be compared with the corresponding observed values, the models' performance improves significantly. The same aggregating effect also explains why the model's performance better at the downstream stations monitoring larger upstream areas.

The SWAT model has a slight better overall performance in reproducing the daily flow values than GWLF, but this comparative advantage is not clearly shown at a monthly time step, showing that the effort in required to calibrate, validate and run more complete and distributed models may not pay off. When detailed precipitation data is not available, simpler lumped models may lead to equally accurate results.

When estimating sediment yield, the models can reproduce the order of magnitude and the major variations of the sediment yield, although not with significant accuracy. The model's performance to reproduce N and P loads is poor, in particularly the nitrogen loads. As the phosphorus loads are better correlated with sediments yield, the model estimates are slightly better when compared

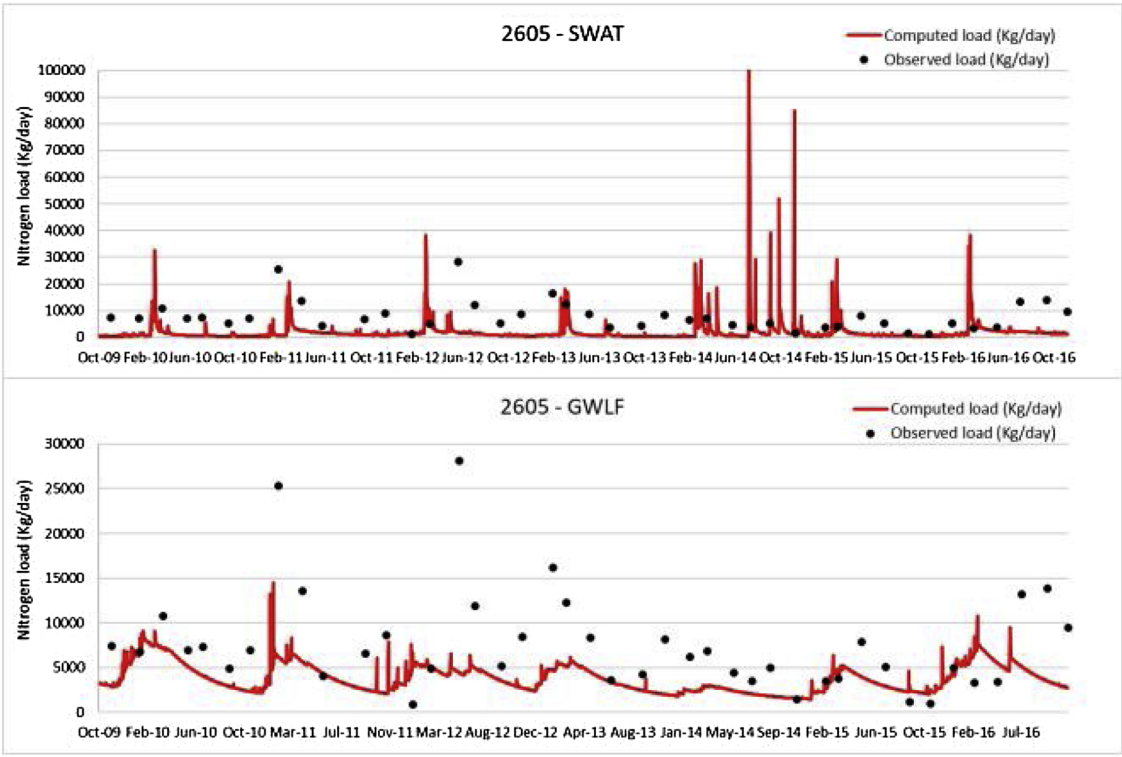

Fig. 10. Performance of SWAT and GWLF models for total nitrogen load at station 2605 (Atibaia river basin).

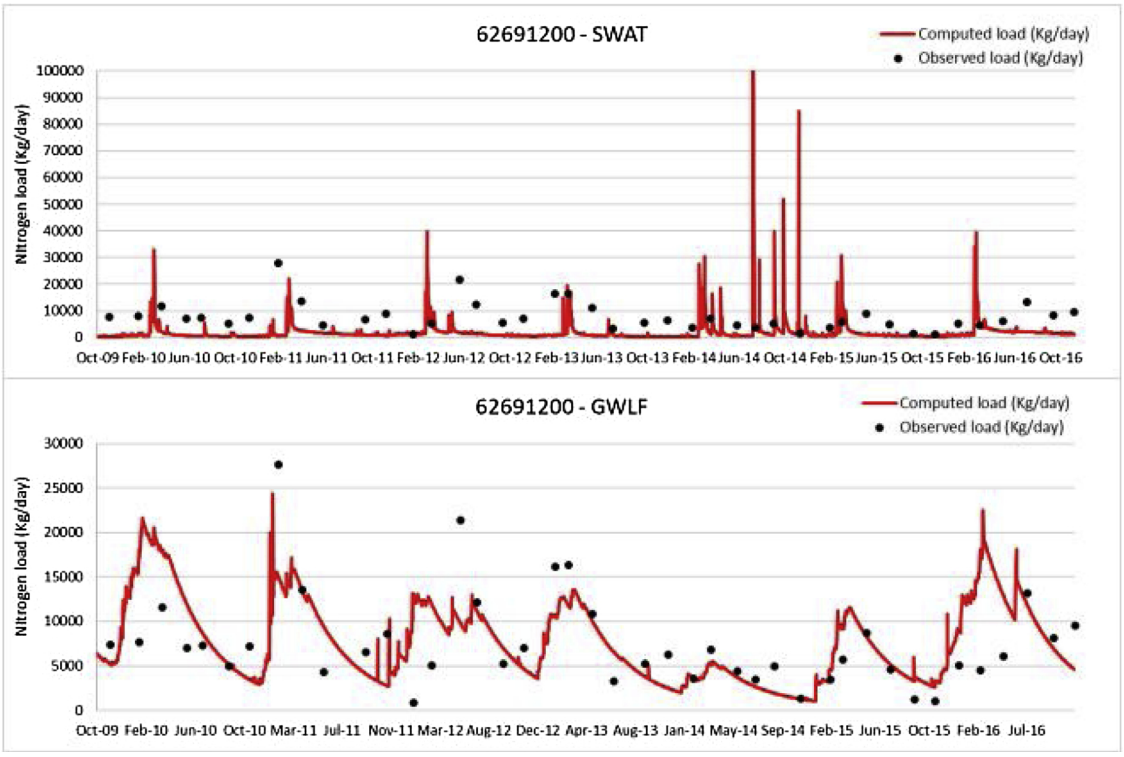

Fig. 11. Performance of SWAT and GWLF models for total nitrogen load at station 62691200 (Atibaia river basin).

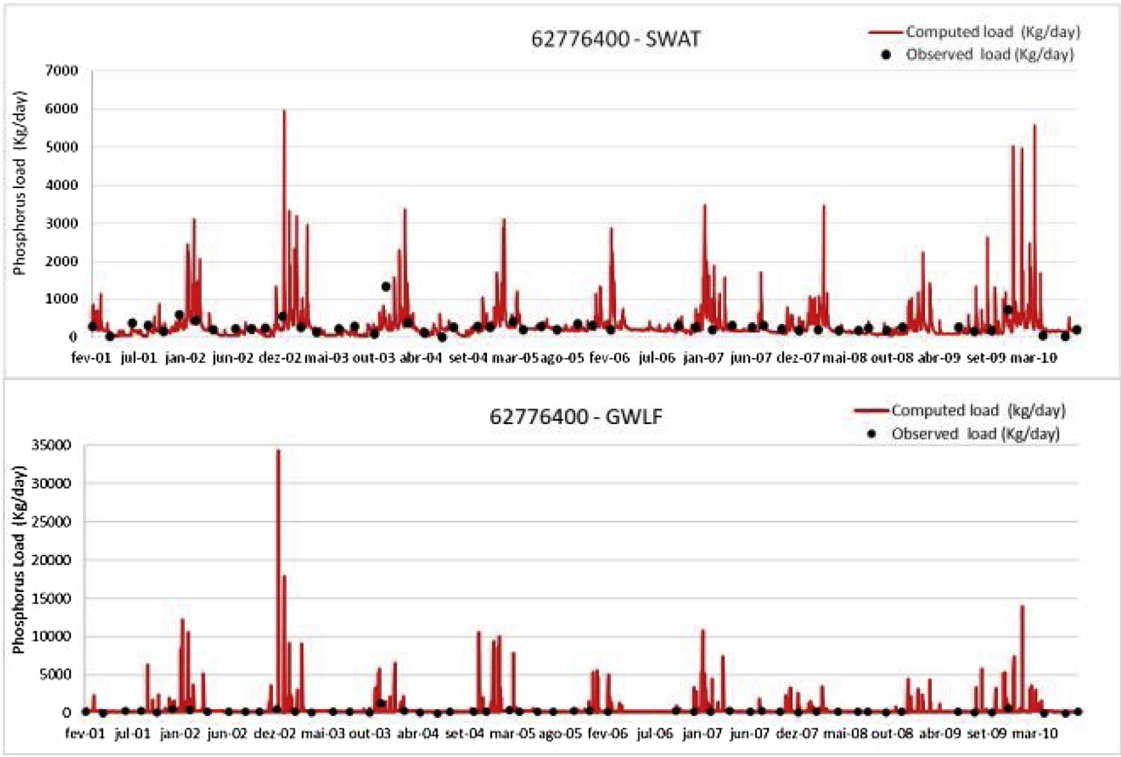

Fig. 12. Performance of SWAT and GWLF models for total phosphorus load at station 62776400 (Atibaia river basin).

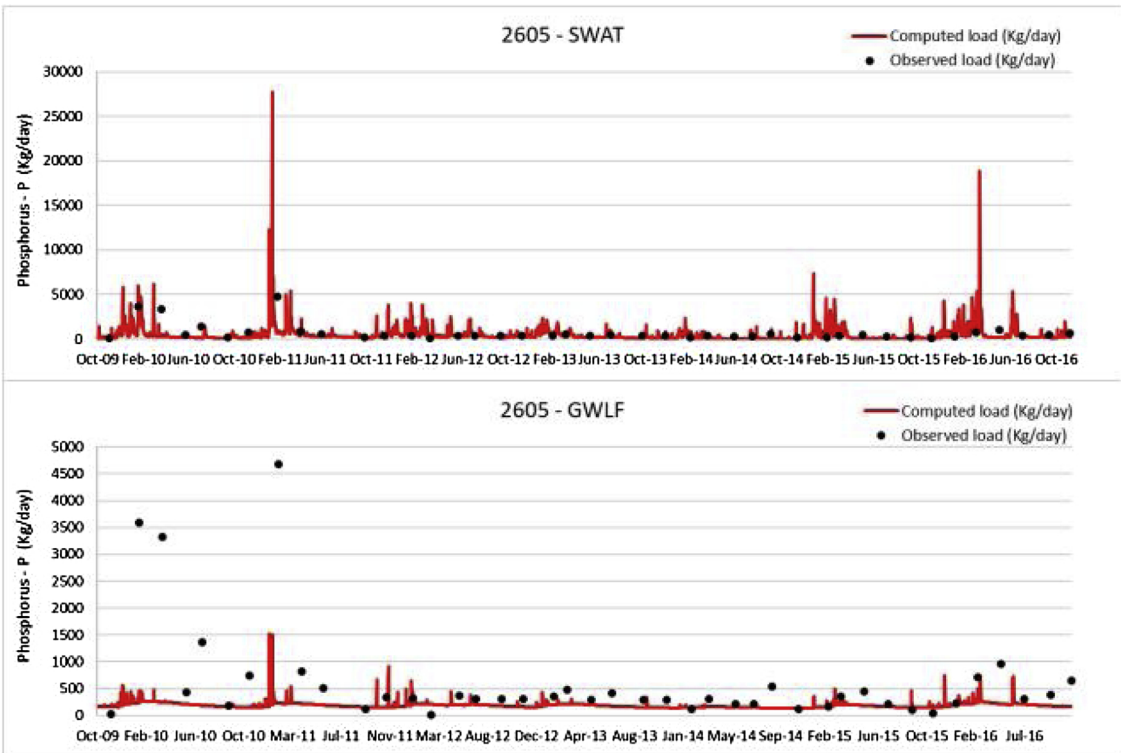

Fig. 13. Performance of SWAT and GWLF models for total phosphorus load at station 2605 (Atibaia river basin).

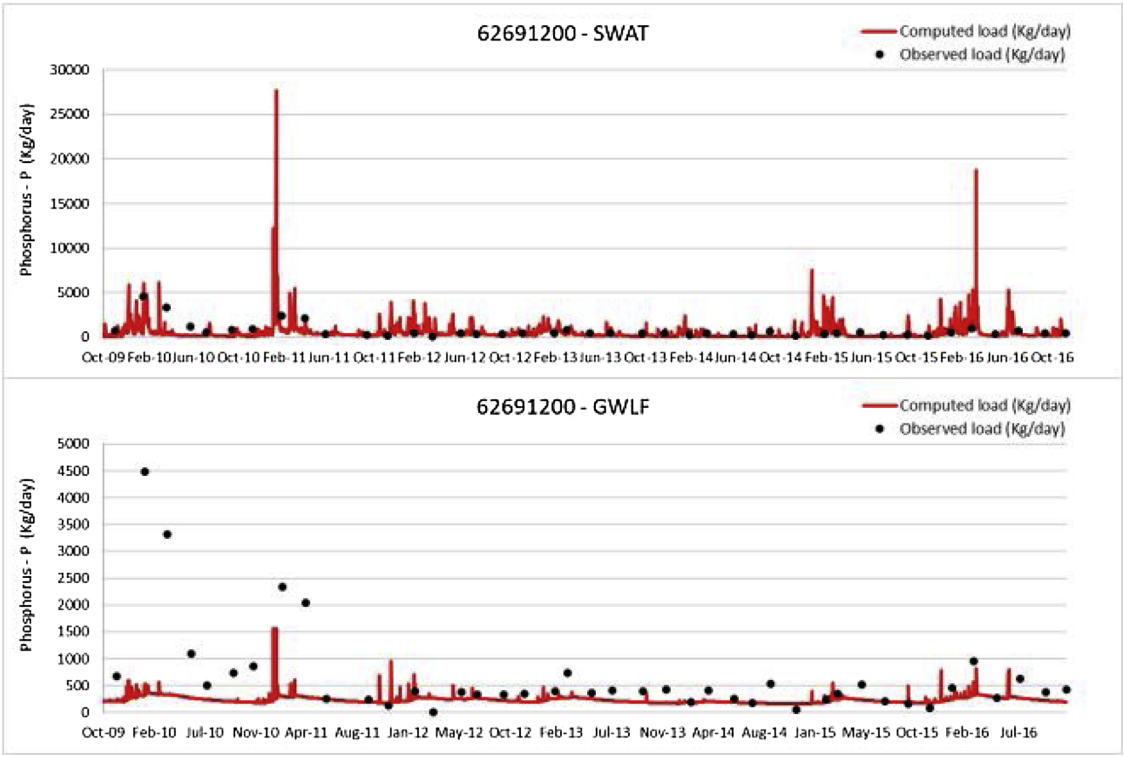

Fig. 14. Performance of SWAT and GWLF models for total phosphorus load at station 62691200 (Atibaia river basin).

with the observed values. Once again, the SWAT performance to estimate sediment, nitrogen and phosphorus loads is slightly better than GWLF, but this comparative advantage may not compensate the additional effort calibrate and validate it.

Models are useful for decision making if they can capture the main signals of the hydrological processes, even if they do not accurately reproduce the finer variability of some variables. Our research showed that GWLF model is a useful decision support tool for preliminary studies at a monthly time step, given the straightforwardness to calibrate and apply the model. When detailed data is available and when estimates are needed for shorter time periods and smaller and more diverse areas, SWAT ability to simulate watershed processes in detail has the potential to lead to better results, if an adequate dataset is available to calibrate and validate the model. And given its more complete and physically based formulation, SWAT is also expected to produce robust results and perform better at situations not used during its calibration.

The research showed that when there are weaknesses in the existing dataset for model calibration and validation, both a more complete model (SWAT) and a parsimonious model (GWLF) fail to reproduce the finer variability of some variables at a daily time step, namely streamflow, sediment loads and nutrients concentration. In such cases, a sensitivity analysis of the input variables and the model parameters may help convey an indication of the model's results uncertainty.

The research also put in evidence some results than can be used to improve the model's performance. SWAT methods to estimate areal average areal precipitation over each HRU could be improved. Concerning GWLF, the use of the original the Soil Conservation Service method (SCS-CN) by GWLF for estimating runoff leads to a highly variable time series that often overestimates flow peaks and total flow volume and the use of the USLE equation with rainfall intensity representing the erosive factor and the non-consideration of erosion and deposition along the main channel also leads to highly variables sediment and phosphorus loads estimates. In the future, it may be possible to improve GWLF formulation to confront these problems and improve is performance, while maintaining the models' parsimony.

Funding

The research is funded by CNPq - Conselho Nacional de Desenvolvimento Científico e Tecnológico, Brazil. ID: 140728/2014-7. SMART^2 Project Smart Cities & Smart Grids for Sustainable Development, Europe. ID: SS15DM0235.

References

Abbaspour, K.C., et al., 2007. Modelling hydrology and water quality in the pre-alpine/alpine Thur watershed using SWAT. J. Hydrol. 333 (2), 413–430.
ABNT - Associação Brasileira de Normas Técnicas, NBR nº 12209, 2011. Dispõe sobre elaboração de projetos hidráulico-sanitários de estações de tratamento de esgotos sanitários. Secretaria de administração do Ministério Público 20/08/2012.

Ajami, N.K., et al., 2004. Calibration of a semi-distributed hydrologic model for streamflow estimation along a river system. J. Hydrol. 298 (1–4), 112–135.
Alkimim, A., Sparovek, G., Clarke, K.C., 2015. Converting Brazil's pastures to cropland: an alternative way to meet sugarcane demand and to spare forestlands. Appl. Geogr. 62, 75–84.
Amy, G., et al., 1974. Water Quality Management Planning for Urban Runoff. U.S. Environmental Protection Agency, Washington DC.
Arnold, J.G., Fohrer, N., 2005. SWAT2000: current capabilities and research opportunities in applied watershed modelling. Hydrological Processes: An International Journal 19 (3), 563–572.
Arnold, J.G., et al., 2012. SWAT: model use, calibration, and validation. Trans. Asabe 55 (4), 1491–1508.
Arnold, J.G., et al., 1998. Large-area hydrologic modeling and assessment: part 1. Model development. J. American Water Resources Assoc 34 (1), 73–89.
Bagnold, R.A., 1977. Bedload transport in natural rivers. Water Resour. Res. 13 (1), 303–312.
Benham, B.L., et al., 2006. Modeling bacteria fate and transport in watershed models to support TMDLs. Trans. ASABE 49 (4), 987–1002.
Beven, K., 2001. How far can we go in distributed hydrological modelling? Hydrol. Earth Syst. Sci. Discuss. 5 (1), 1–12.
Bonumá, N.B., Rossi, C.G., Arnold, J.G., 2013. Hydrology evaluation of the soil and water assessment tool considering measurement uncertainty for a small watershed in Southern Brazil. Appl. Eng. Agric. 29 (2), 189–200.
Caldwell, P.V., et al., 2015. A comparison of hydrologic models for ecological flows and water availability. Ecohydrology 8 (8), 1525–1546.
Chow, V.T., 1959. Open Channel Hydraulics. McGraw-Hill, New York, N.Y 680 pp.
Coffey, S.R., Workman, J.L., Taraba, A.W., 2004. Fogle Statistical procedures for evaluating daily and monthly hydrologic model predictions Trans. ASAE 47 (1), 59–68.
Comitê das Bacias Hidrográficas dos rios Piracicaba, Capivari e Jundiaí (CBH-PCJ), 2006. Plano de Bacias Hidrográficas 2004-2007 dos rios Piracicaba, Capivari e Jundiaí. Relatório Final. Disponível em. Acesso em: 10 mar. 2017. www.comitepcj.sp.gov.br.
Devia, G.K., Ganasri, B.P., Dwarakish, G.S., 2015. A review on hydrological models. Aquat. Procedia 4, 1001–1007.
Du, X., Li, X., Zhang, W., Wang, H., 2014. Variations in source apportionments of nutrient load among seasons and hydrological years in a semi-arid watershed: GWLF model results. Environ. Sci. Pollut. Res. - Int. 21 (10), 6506–6515.
Fatichi, S., et al., 2016. An overview of current applications, challenges, and future trends in distributed process-based models in hydrology. J. Hydrol. 537 (1), 45–60.
Francesconi, W., et al., 2016. Srinivasan, Raghavan, Perez-Miñana, Elena., Willcock, Simon P., Quintero, Marcela, using the soil and water assessment tool (SWAT) to model e.cOsystem services: a systematic review. J. Hydrol. (Amst) 535 (1), 625–636.
Freire, O., et al., 1978. Solos da bacia do Broa. Univ. Fed. São Carlos, São Paulo 125p.
Gitau, M.W., Chaubey, I., 2010. Regionalization of SWAT model parameters for use in ungauged watersheds. Water 2 (4), 849–871.
Gupta, H.V., Wagener, T., Liu, Y., 2008. Reconciling theory with observations: elements of a diagnostic approach to model evaluation. Hydrol. Process. 22 (18), 3802–3813.
Haith, D.A., Shoemaker, L.L., 1987. Generalized watershed loading functions for stream flow nutrients. Water Resources Bulletin 23 (3), 471–478.
Haith, D.A., Mandel, R., Wu, R.S., 1992. Generalized Watershed Loading Functions Version 2.0 User's Manual. Cornell University, Ithaca, New York.
Hajigholizadeh, M., Melesse, A., Fuentes, H., 2018. Erosion and sediment transport modelling in shallow waters: A review on approaches, models and applications. Int. J. Environ. Res. Public Health 15 (3), 518.
Huang, J., Hong, H., 2010. Comparative study of two models to simulate diffuse nitrogen and phosphorus pollution in a medium-sized watershed, southeast China. Estuar. Coast. Shelf Sci. 86 (3), 387–394.
Huber, W.C., Dickinson, R.E., 1988. Storm Water Management Model, Version 4: User's Manual. Cooperative agreement. U.S. Environmental Protection Agency, Athens, GA.
Klemeš, V., 1986. Operational testing of hydrological simulation models. Hydrol. Sci. J. Des Sci. Hydrol. 31 (1), 13–24.
Krause, P., Boyle, D.P., Bäse, F., 2005. Comparison of different efficiency criteria for hydrological model assessment. Adv. Geosci. 5 (1), 89–97.
Lee, K.Y., et al., 2000. Modeling the hydrochemistry ofthe Choptank River basin using GWLF and GIS. Biogeochemistry 49 (1), 143–173.
Lenhart, K., Eckhardt, N., Fohrer, F.H.G., 2002. Comparison of two different approaches of sensitivity analysis. Phys. Chem. Earth 27 (1), 645–654.
Li, Z., Xu, Z., 2011. Performance of WASMOD and SWAT on hydrological simulation in Yingluoxia watershed in northwest of China. Hydrol. Process. 25 (13), 2001–2008.
Li, X., Weller, D.E., Jordan, T.E., 2010. Watershed model calibration using multi-objective optimization and multi-site averaging. J. Hydrol. 380 (3), 277–288.
Lombardi Neto, F., et al., 1989. Nova abordagem para cálculo de espaçamento entre terraços. In: Neto, Lombardi, Jr, Belinazzi (Eds.), Simpósio Sobre Terraceamento Agrícola. Fundação Cargill, Campinas, pp. 99–124.
Malagó, A., et al., 2017. Modelling water and nutrient fluxes in the Danube River Basin with SWAT. Sci. Total Environ. 603 (1), 196–218.
Me, W., Abell, J.M., Hamilton, D.P., 2015. Effects of hydrologic conditions on SWAT model performance and parameter sensitivity for a small, mixed land use catchment in New Zealand. Hydrol. Earth Syst. Sci. 19 (10), 4127.
Madsen, H., 2000. Automatic calibration of a conceptual rainfall–runoff model using multiple objectives. J. Hydrol. 235 (3–4), 276–288.
Mirchi, A., Watkins Jr., D.W., Madani, K., 2010. Modeling for watershed planning, management and decision making. In: Vaughn, J.C. (Ed.), Watersheds Management, Restoration and Environmental Impact. Nova, Hauppauge, New York.
Michaud, J., Sorooshian, S., 1994. Comparison of simple versus complex distributed runoff models on a midsized semiarid watershed. Water Resour. Res. 30 (3), 593–605.
Monteiro, J.A., 2016. Accuracy of grid precipitation data for Brazil: application in river discharge modelling of the Tocantins catchment. Hydrol. Process. 30 (9), 1419–1430.
Moriasi, D.N., et al., 2007. Model evaluation guidelines for systematic quantification of accuracy in watershed simulations. Trans. Asabe 50 (3), 885–900.
Naef, F., 1981. Can we model the rainfall-runoff process today? Hydrol. Sci. J. Des Sci. Hydrol. 26 (3), 281–289.
Nash, J.E., Sutcliffe, J.V., 1970. River flow forecasting through conceptual models part I—a discussion of principles. J. Hydrol. 10 (3), 282–290.
Neitsch, S.L., et al., 2002. Soil and Water Assessment Tool User's Manual: Version 2000. GSWRL Report 02-02, BRC Report 02-06. Texas Water Resources Instititue, TR-192, College Station, Texas 438p.
Neitsch, S.L., et al., 2005. Soil and Water Assessment Tool Theoretical Documentation. Grassland. Soil and Water Research Laboratory, Temple, TX.
Neitsch, S.L., et al., 2001. Soil and Water Assessment Tool, Theoretical Documentation. Version 2000. Blackland Research Center, Texas Agricultural Experiment Station, Temple, Texas.
Neitsch, S.L., et al., 2009. Soil and Water Assessment Tool Theoretical Documentation Version 2009. Texas Water Resources Institute.
Neitsch, S.L., et al., 2011. SWAT Model User's Manual. Texas A&M University, Texas.
Nejadhashemi, A.P., Wardynski, B.J., Munoz, J.D., 2012. Large-scale hydrologic modeling of the michigan and wisconsin agricultural regions to study impacts of land use changes. T. ASABE 55 (1), 821–838.
Niraula, R., 2013. Identifying critical source areas of nonpoint source pollution with SWAT and GWLF. Ecol. Modell. 268 (1), 123–133.
Oliveira, J.B., Prado, H., 1984. Levantamento Pedológico Semidetalhado Do Estado De São Paulo. IAC, Memorial descritivo. Campinas 110p.
Parajuli, P.B., et al., 2009. Comparison of AnnAGNPS and SWAT model simulation results in USDA-CEAP agricultural watersheds in south-central Kansas. Hydrological Processes: An International Journal 23 (5), 748–763.
Pontes, L.M., et al., 2016. Hydrological modeling of tributaries of cantareira system, Southeast Brazil, with the Swat model. Engenharia Agrícola 36 (6), 1037–1049.
Qi, Z., et al., 2017. Comparison of SWAT and GWLF model simulation performance in humid south and semi-arid north of China. Water 9 (8), 567.
Quilbé, R., et al., 2006. Selecting a calculation method to estimate sediment and nutrient loads in streams: application to the Beaurivage River (Québec, Canada). J. Hydrol. 326 (1–4), 295–310.
Rabelo, J., Quaresma, E., Wendland, E., 2004. Modelo conceitual de área de afloramento do Aquífero Guarani na região central do estado de São Paulo. *In:* Anais do XIII Congresso Brasileiro de Águas Subterrâneas. Cuiabá.
Santos, F.M., de Oliveira, R.P., Mauad, F.F., 2018. Lumped versus distributed hydrological modeling of the Jacaré-Guaçu Basin, Brazil. J. Environ. Eng. 144 (8),

0401–8056.
Sartor, J.D., Boyd, G.B., 1972. Water Pollution Aspects of Street Surface Contaminants. U.S. Environmental Protection Agency, Washington DC 1972.
Saxton, K.E., Rawls, W.J., 2006. Soil water characteristic estimates by texture and organic matter for hydrologic solutions. Soil Sci. Soc. Am. J. 70 (5), 1569–1578.
Schneiderman, E.M., et al., 2002. Modeling the hydrochemistry of the Cannonsville watershed with Generalized Watershed Loading Functions (GWLF). JAWRA Journal of the American Water Resources Association 38 (5), 1323–1347.
Strauch, M., et al., 2013. The impact of Best Management Practices on simulated streamflow and sediment load in a Central Brazilian catchment. J. Environ. Manage. 127 (1), 24–36.
Strassburg, B.B., et al., 2017. Moment of truth for the Cerrado hotspot. Nat. Ecol. Evol. 1 (4), 99.
Swaney, D.P., Sherman, D., Howarth, R.W., 1996. Modeling water, sediment and organic carbon discharges in the Hudson–Mohawk basin. Estuaries 19 (4), 833–847.
Tu, J., et al., 2009. Combined impact of climate and land use changes on stream- flow and water quality in eastern Massachusetts, USA. J. Hydrol. 379 (3–4), 268–283.
Vanoni, V.A., 1975. Sedimentation Engineering, Chapter 4, Sediment Sources and Sediment Yields. American Society of Civil Engineers, Reston, pp. 437–493.
Wilcox, B.P., et al., 1990. Predicting runoff from rangeland catchments: a comparison of two models. Water Resour. Res. 26 (10), 2401–2410.
Williams, J.R., 1975. Sediment routing for agricultural watersheds. Water Resour. Bull. 11 (5), 965–974.
Wischmeier, W.H., Smith, D.D., 1978. Predicting Rainfall Erosion losses – a Guide to Conservation Planning. USDA Agriculture Handbook No. 537. U.S. Government Printing Office, Washington, D.C.
Wu, W., Hall, C.A.S., Scetena, F.N., 2007. Modeling the impact of recent landuse changes on the stream flows in northeastern Puerto Rico. Hydrol. Process. 21 (1), 2944–2956.
Yilmaz, K.K., Gupta, H.V., Wagener, T., 2008. A process-based diagnostic approach to model evaluation: application to the NWS distributed hydrologic model. Water Resour. Res. 44 (9).
Young, P.C., Parkinson, S., Lees, M., 1996. Simplicity out of complexity in environmental modelling: occam's razor revisited. J. Appl. Stat. 23 (2–3), 165–210.